Review Article

Recent Progress of Advanced Metal-Oxide Nanocomposites for Effective and Low-Cost Antimicrobial Activates: A Review

Ruth Birhanu,[1] Mesfin Asfaw Afrasa,[1] and Fekadu Gashaw Hone [2]

[1]*Department of Applied Physics, Adama Science and Technology University, P. O. Box 1888, Adama, Ethiopia*
[2]*Department of Physics, Addis Ababa University, P. O. Box 1176, Addis Ababa, Ethiopia*

Correspondence should be addressed to Fekadu Gashaw Hone; fekeye@gmail.com

Pathogens with multidrug resistance have recently been responsible for widespread disease, fatalities, and economic distress. A nanomaterial with antibacterial characteristics is used to reduce the infection's resistance. Metal-oxide nanocomposites are nanomaterials that exhibit outstanding physical and chemical characteristics. They are prime candidates for innovative functional materials with antimicrobial activity as one of their main uses. This review will summarize the current progress on the antimicrobial activity of metal-oxide nanocomposite, including widely recognized research outputs and recent findings, as these materials can overcome the limitation of the individual material due to their utterly different properties from the single materials. Additionally, it describes several metal-oxide nanocomposites that are produced using various methods for the application of antimicrobial activity, as well as the variables that can affect such activities and the main inhabitation mechanisms of this materials.

1. Introduction

An individual or population has become infected when pathogenic germs have invaded and started to multiply there. Antibiotics are made to prevent the manufacture of bacterial cell walls, proteins, deoxyribonucleic acid (DNA), and other biological processes without being hazardous to nearby tissue to stop bacterial development. Recently, microbial contamination is a significant issue in clinical or hospital settings, medical devices, cleaning supplies, water purification systems, textiles, food packaging, and food storage [1–3]. These are brought on by their intricate growth and fast genomic changes for antibiotic adaptation [4]. This is an indication from a report on US healthcare released in 2019 that the result is 2.8 million diseases, 35,900 fatalities per year, and at least USD 20 billion in costs [5]. Therefore, scientists started to develop drugs that are very powerful against a variety of bacterial systems, making it more difficult for the bacteria to develop resistance to them. One way to address the gaps left by antibiotics is with antimicrobial nanoscale materials [6]. Nanoparticles (NPs) frequently operate at the lowest levels, have a broad antimicrobial

spectrum at short contact times, are affordable and easy to prepare, are highly stable in their intended applications and storage, regenerate after losing their efficacy, and enter the ecosystem's food chain directly [3, 7]. This antibacterial compound works against fungus, viruses, and protozoa in addition to bacteria. Antibacterial NPs (AMNPs) are nanomaterials having antimicrobial capabilities [8]. Due to the way they hinder the bacterial cell, NPs with antibacterial properties are more advantageous and effective than antibiotics. NPs attack the bacterium by rupturing the cell wall/membrane, interacting with DNA and proteins, interrupting electron transport, and altering the bacterial redox state. In contrast to antibiotics, it can stop the growth of bacteria by preventing the creation of target biomolecules in bacteria like cell walls, DNA, proteins, etc. [9]. However, the physicochemical properties of NPs, such as their size, shape, chemical modifications, coatings, and combinations in various ratios with other NPs and solvents, all have an impact on the antibacterial activity of antimicrobial peptides [10–12]. To put it simply, as NP's size reduces, its surface area grows, increasing its antimicrobial effectiveness since it creates more active atomic surfaces and raises the risk of
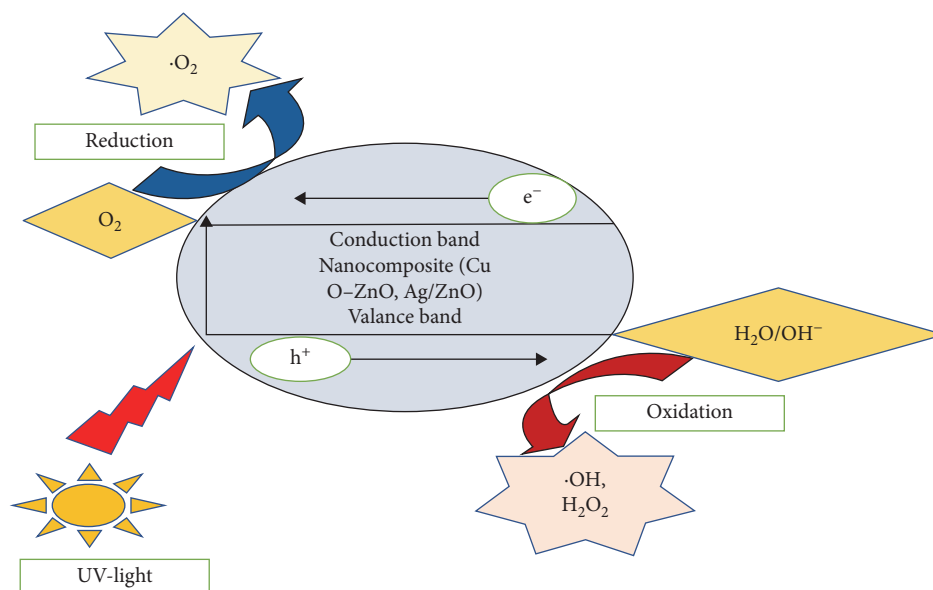
FIGURE 1: Mechanism of ROS generation on the surface of a give nanocomposites (adapted from [28]).

exposure to microbes [13, 14]. Metal, metal oxide, and organic NPs are currently used as antimicrobial application. Numerous metal-oxide nanoparticles (MONPs), including CuO, ZnO, TiO_2, SnO_2, Mn_3O_4, Fe_2O_3, and MgO, have been created and tested for antimicrobial activity against a variety of pathogenic bacterial strains [15] because of their improved durability, lower toxicity, higher stability, heat resistance, should not react with food or containers, have a good taste or no taste, and provide mineral elements necessary for human cells [16, 17]. Nowadays, nanocomposites are frequently used to boost the efficacy of antimicrobial activity because of their narrow size distribution, efficient compositions, stability, longer life, reduced toxicity of the NPs, microscopic size, and nondispersive, nonaggregative, and nonagglomerative properties [18–20]. A subset of composite materials known as nanocomposites can be created artificially or naturally and consist of one or more phases with at least one dimension of order 100 nm or less, with the majority of solid phases falling between 1 and 20 nm [21]. They have better qualities than the original materials when used in a particular finished structure; this is because they combine two or more separate constituent elements, each of which has a unique significant property (physical or chemical) [22, 23]. In addition to regulate structure and size, different preparation procedures have been used to generate nanocomposite materials. A narrow size distribution, control of particle shape, reduction of particle size, and crystallite management are the fundamental objectives of particle synthesis. Characterization is crucial for properly comprehending and assessing size distributions, composition, the level of aggregation, surface area, and surface chemistry. It also helps to identify the application for which we must employ the material [24]. Similar to other NPs, nanocomposites contain unique pathways for bacterial inhabitation. The two main methods, a nanocomposite utilized to suppress the bacterial cell, are depicted in Figures 1 and 2.

(1) Nanocomposite may interact directly with the bacterial cell membrane by electrostatic interactions between the ions released and the negatively charged bacterial cell wall [25] or by releasing heavy metal ions upon surface oxidation [26]

(2) By activating the nanocomposite with UV light and increasing electron–hole pairs to generate reactive oxygen species (ROS), including hydrogen peroxide (H_2O_2), hydroxyl radical (OH), singlet oxygen (O_2), and superoxide anion (O_2^-), they are created that can directly harm the bacteria's DNA, lipids, and proteins, killing the organism [27]. In this paper, we review relevant research on metal-oxide nanocomposites, which are useful for antimicrobial activities, as well as the difficulty (factor) that can restrict the inhabitation of metal-oxide nanocomposites against the multidrug resistance bacterial and inhabitation mechanisms of metal-oxide nanocomposites. We think that this study will help researchers interested in the currently hot topic of the antibacterial activities of metal-oxide nanocomposites that gain a general understanding of the subject and identify effective mitigating tactics for these difficulties

2. Metal Oxides for Antimicrobial Activity

Metals can form oxides by combining at least one metal cation and an oxygen anion adopting a wide range of structural geometries and exhibiting metallic, semiconductor, or insulating properties. The appropriate manipulation of these materials is at the nanoscale and the production of MONPs [30, 31]. Engineered MONPs find extensive use in a variety of fields, including catalysis, sensors, (opto)electronic materials, environmental remediation, antibacterial agents in clothing and cosmetics, biomedicine, and food additives.
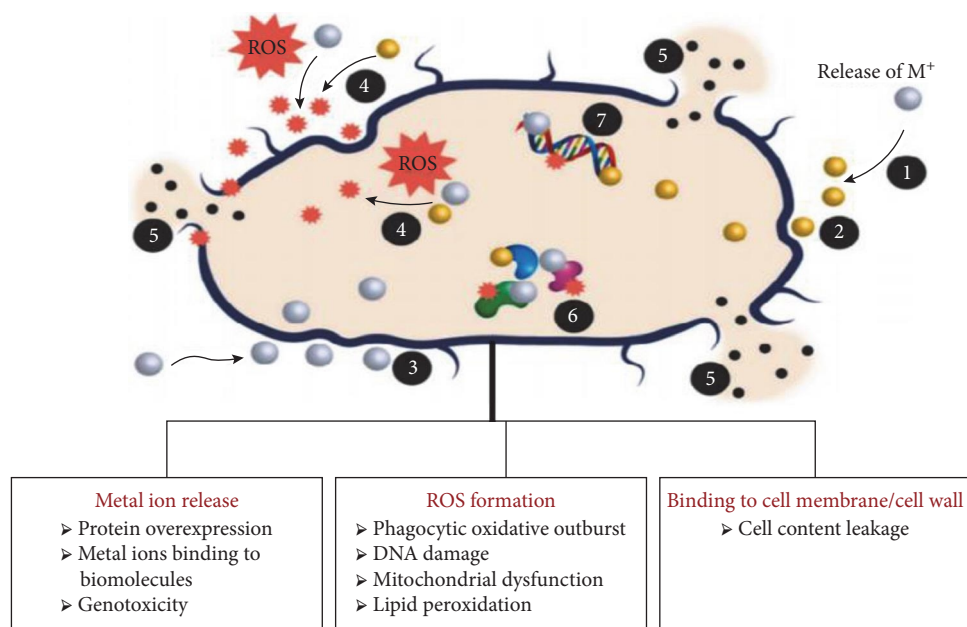
FIGURE 2: Antibacterial mechanisms of metal ions and nanocomposites. The central modes of action are: (1) release of metal ions from the metal nanoparticles and (2) direct interaction of the metal ions and/or (3) metal nanoparticles with the cell wall through electrostatic interactions, leading to impaired membrane function and impaired nutrient assimilation; (4) formation of extracellular and intracellular reactive oxygen species (ROS), and damage of lipids, proteins and DNA by oxidative stress; (5) high-levels of metal-binding to the cell envelope and high ROS levels can cause damage to the plasma membrane and thus lead to the leakage of the cell content; (6, 7) upon metal uptake, metal nanoparticles and metal ions can directly interfere with both proteins and DNA, impairing their function and disturbing the cellular metabolism in addition to metal mediated ROS production (adapted from [29]).

They differ greatly from the analogous bulk material due to their nanoscale physiochemical properties, which include their optical, thermal, electrical, surface area-to-volume ratio, surface charge, catalytic activity, antibacterial properties, magnetic properties, and reactivity [32–38].

Recently, there has been a lot of interest in the study, design, synthesis, and characterization of various metallic NPs for the treatment and targeting of many diseases [39]. Since they have better durability, lower toxicity, higher stability, and stronger heat resistance, various metallic NPs have recently attracted a lot of attention for the treatment and targeting of many diseases. They also supply mineral elements that are crucial for human cells [17]. To examine the antibacterial properties of various MONPs, numerous researchers manufacture these materials. This is a result of their ions' capacity to block enzymes, promote the production of ROS, damage cell membranes, limit microbial uptake of critically needed microelements, and exert direct genotoxic activity in some metals [40]. The antibacterial capabilities of metal and MONPs, such as silver, zinc, copper, zinc oxide, titanium dioxide, copper oxide, and iron oxide, are known to be demonstrated against different bacterial strains. For those NPs' bactericidal properties, several methods have been put forth. These include: (1) the destruction of the bacterial cell membrane and electron transport chain; (2) the production of ROS and induction of oxidative stress as a result of the interaction of NPs with the bacterial cell membrane and cellular components such as DNA and protein; and (3) released metal ions from metal or MONPs in the intracellular environment [41].

3. Nanocomposites

For indubitable purposes, engineers often ask for innovative material systems. In response, material scientists are required by this demand to create novel composite material systems with explicit strength and stiffness, corrosion resistance, low density, and high thermal insulation [42]. In complex technology, a novel functional material is created by fusing two or more chemically detached materials or phases, so that the individual components remain distinct and recognizable. By masking the original material's flaws, composites enable new materials to combine the strengths of both types of material [43, 44]. They have essentially three phases to these materials. The initial, continuous phase is referred to as the matrix, which is the softest and more ductile phase. It shares a load with the scattered juncture and holds it. The scattered phase was the second phase (or phases), which is a continuous/discontinuous shape embedded in the matrix. Since the scattered juncture typically outperforms the matrix in strength, it is referred to as the reinforcing phase. The zone where the matrix phase and reinforcing phase interact via chemical, physical, mechanical, electrical, and other processes is known as the interface. Due to chemical or diffusional interactions between the fiber and matrix, this region of composite materials has a finite thickness [45, 46]. A multiphase solid substance called "nanocomposite" having one, two, or three dimensions on the nanometer scale or less than 100 nm has more than one phase. Due to the nanometric size effect and the material's multifunctionality, nanocomposite materials can exhibit different mechanical, electrical, optical,
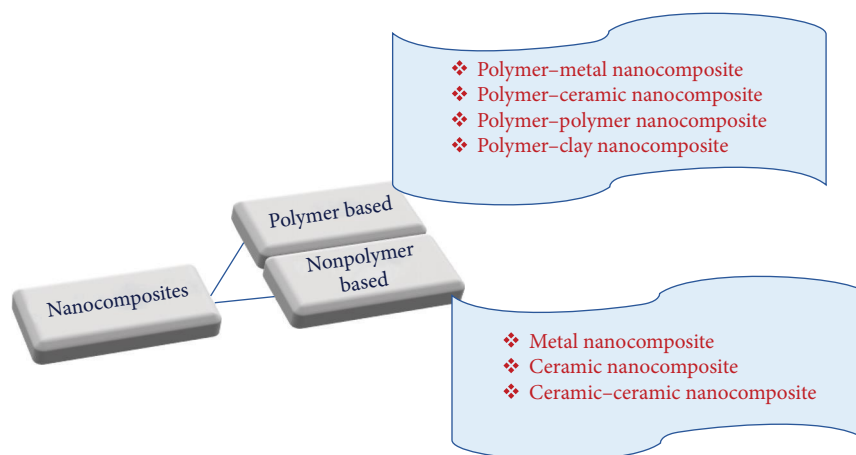
FIGURE 3: Schematic diagram representing classification of nanocomposites (adapted from [51]).

FIGURE 4: Diagram of different synthesis methods of nanocomposites (adapted from [56]).

electrochemical, catalytic, and structural properties than those of each component [47, 48]. Each structure and feature of the several phases are merged throughout the nanocomposite formation process to create hybrid materials that have multiple functionalities in terms of both structure and material properties [49]. Based on whether or not there is polymeric material in the composite, nanocomposite materials can be categorized in the ways listed below. Nonpolymer-based nanocomposites are those in which the compositions do not contain any polymers or materials produced from polymers. The second type is a nanocomposite in which the formation does accommodate polymer [50]. Their subsequent classification is shown in Figure 3.

4. Antimicrobial Activates of Nanocomposites

Microorganisms can develop resistance to several antibiotics. Recently, bacterial resistance has increased, necessitating the urgent need for a new therapeutic agent that is benign to humans but lethal to microorganisms. Therefore, the creation of antibacterial drugs mediated via nanocomposite is highly warranted. Any type of chemical or physical substance that can treat, eliminate, or stop the spread of microorganisms

(bacteria, fungus, viruses, and protozoans) over the world is referred to as an antimicrobial agent [52]. Numerous assay techniques, including well diffusion (WD), disk diffusion, and agar dilution methods, are used to assess the antimicrobial activity of synthesized nanocomposites. However, other techniques, like bioluminescent and flow cytofluorometric methods, are less popular because they call for specialized equipment [53]. The antimicrobial potency of the sample, which is measured by this assay method as the minimal concentration of inhibition against the targeted bacterial strains, is determined or indicated. The lowest dose of an antimicrobial agent required to kill 99.9% of the final inoculum, predict antibacterial activity in vitro or impede the visible growth of a bacterium, is known as the minimum inhibitory concentration (MIC) [54, 55]. Nanocomposites must first be manufactured before they can be used for antibacterial action. Various techniques can be used to create nanocomposites, as demonstrated in Figure 4. Nanocomposites can be characterized using methods that are nearly identical to those used for NPs.

4.1. Mixed Metal-Oxide Nanocomposites for Antibacterial Activities. By blend two or more metal oxides (p- and n-type semiconductors) chemically or physically, mixed
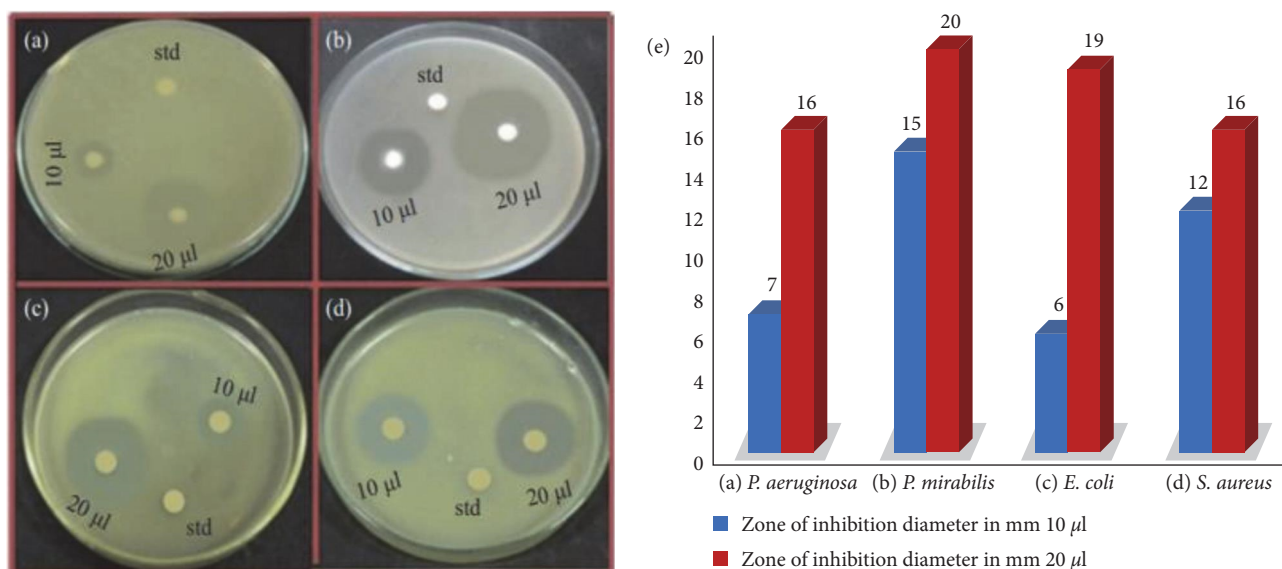
FIGURE 5: Inhibition zone produced by ZnO–CuO nanocomposite (3 : 1 M) for (a) *P. aeruginosa*, (b) *P. mirabilis*, (c) *E. coli*, and (d) *S. aureus*. (e) bar graph representing the size of the zone of inhibition formed around each disk, loaded with test samples, indicating the antibacterial activity toward the same for ZnO–CuO nanocomposite 3 : 1 M (adapted from [62]).

MONPs are created. In contrast to the individual metal oxides, these exhibit distinct physicochemical traits [18, 57]. Most scientists are currently investigating the antibacterial activity of these nanocomposites on various bacterial infections using numerous synthesis techniques. Mixed metal-oxide nanocomposites were created synthetically and are being examined by countless writers. In 2015, Subhan et al. synthesized mixed metal-oxide nanocomposite NiO–CeO$_2$–ZnO and CeO$_2$–CuO–ZnO for antibacterial and photocatalytic activities [58, 59]. Mixed metal oxides have been widely employed as antibacterial agents in recent years. Sudhaparimala and Vaishnavi [60] created SnO$_2$–ZnO with and without *Aloe vera* plant as the medium using a simple and environmentally friendly sol–gel synthesis method. At doses of 100, 200, and 300 μg, an *A. vera* plant-based nanocomposite exhibits strong antibacterial activity against *Staphylococcus aureus* with zones of inhabitation of 17, 21, and 24 mm and against *Escherichia coli* with zones of inhabitation of 20, 23, and 25 mm. The sample that did not use the *A. vera* plant as a substrate was unable to maintain bacterial growth [60]. In 2018, Mohammadi-Aloucheh et al. produced ZnO from zinc(II) nitrate precursor and ZnO/CuO nanocomposite from *Vaccinium arctostaphylos* L. fruit extract. Both bacteria were resistant to the ZnO(W) sample's meager antibacterial action. The percentages of bacteria that were still alive were, however, decreased when ZnO was produced in the presence of *V. arctostaphylos* L. extract. Against both *E. coli* and *S. aureus*, however, the ZnO/CuO nanocomposites showed strong antibacterial activity. When the concentration of CuO was raised, the antibacterial activity of ZnO/CuO nanocomposites was somewhat enhanced. Additionally, the ZnO/CuO nanocomposite's (10%) antibacterial activity against *E. coli* (12.1 ± 0.39) was stronger than that shown with *S. aureus* (14.9 ± 0.65). Compared to ZnO(W), ZnO/CuO nanocomposite is more effective against *E. coli* and *S. aureus* bacterial

strains [61]. In the same year, Saravanakkumar et al. developed the modified perfume spray pyrolysis method (MSP), which they used for the first time, to produce CuO–ZnO nanocomposite with antibacterial activity against *Proteus mirabilis*, *E. coli*, and *S. aureus* bacterial pathogens. With a concentration ratio of CuO/ZnO (3 : 1), the results showed that the maximum zone of inhibition (ZOI) against *P. mirabilis* is 20 mm for 20 L [62]. Figure 5 depicts the area that the prepared sample occupies. Karthik et al. [63] conducted numerous studies on the antimicrobial properties of mixed metal-oxide nanocomposite. In 2018, they used a microwave-assisted technique to create a CdO–NiO–ZnO mixed metal-oxide nanocomposite, which was conducted in vitro to examine the photocatalytic and antibacterial properties of the nanocomposite. They conducted the test against Gram-negative bacteria (*E. coli*, *Pseudomonas aeruginosa*, *P. mirabilis*, *Aeromonas hydrophila*, *Salmonella typhi*, and *Vibrio cholerae*) and Gram-positive bacteria (*S. aureus*, *Rhodococcus rhodochrous*, and *Bacillus subtilis*) at various doses.

The inhabitation zone (16, 25, 26, 24, 26, and 27 nm) for Gram-negative bacteria and (27, 24, and 25 nm) for Gram-positive bacteria had obtained at concentration of 100 g/ml. In their study, three responsible factors for the antibacterial activity of CdO–ZnO–MgO nanocomposite were specified: the release of heavy metal ions, the generation of ROS, and surface morphology. To increase the electron–hole pairs for the production of ROS, CdO–ZnO–MgO nanocomposite has activated by UV light, which led to the production of the electrons on the conduction band and holes on the valence band. The holes that are created can react with water that has adhered to the surface of the CdO–ZnO–MgO nanocomposite to produce hydroxyl radicals (OH), which then collide with electrons to create H$_2$O$_2$ molecules that can pass through the bacterial cell membrane and stop the biological process. Simultaneously, oxygen on the CdO–ZnO–MgO

nanocomposite surface is reduced to a superoxide radical anion (O_2) by generating electrons that lead to the generation of OH. These OH are toxic to the bacterial cell to cause several damages to proteins, lipids, DNA, and profiles of the outer wall of the bacteria, thereby leading to the destruction of the bacteria. The second reason was the ability of CdO–ZnO–MgO nanocomposite to produce heavy metal ions. such as Cd^{2+}, Zn^{2+}, and Mg^{2+} ions that can make attraction with the negatively charged cell membranes and penetrate the cell membrane to react with the sulfhydryl (–S–H) groups and damage the cells' ability to grow through cell division, which leads to the death of the microbe. Third, uneven surface texture of the nanocomposite due to rough edges and corners contributes to the mechanical damage of the cell membrane [63]. In the same year, they created a CdO–ZnO–MgO nanocomposite to explore its photocatalytic and antibacterial properties. Different concentrations of the antibacterial agent were tested in vitro against Gram-negative bacteria such as *E. coli*, *P. aeruginosa*, *V. cholerae*, *Klebsiella pneumoniae*, *Proteus vulgaris*, and *S. typhi*, as well as Gram-positive bacteria such as *B. subtilis*. In their research, the ZOI significantly increases with increasing concentration, and 100 g/ml is the ideal concentration of nanocomposite for preventing the growth of bacterial test organisms [27]. To assess the outcome of lead ions (Pb^{2+}) removal from aqueous solution and antibacterial activity against *S. aureus*, *P. aeruginosa*, and *Candida albicans Trichophyton* fungi at 75 and 100 weight (g) of sample per ml, ur-Rehman et al. [64] produced TiO_2–SnO_2 binary nanocomposite. For both concentrations of the NC, the produced NC exhibits good antibacterial activity against the selected diseases. Similar to the findings of previous researchers, the produced binary nanocomposite's antibacterial activity shows a higher ZOI when concentration rises from 75 to 100 g/ml [64]. Rakesh et al. [65] proposed the low-cost and environmental sustainability zeolite cerium oxide (ZEC) nanocomposite for antibacterial application against *B. subtilis* and *E. coli* bacteria. ZEC was synthesized by the coprecipitation method and assessed using the disk diffusion method. They compared the inhabitation of the prepared nanocomposite by using the work of Alswata et al. as a reference. Their comparison shows that the antibacterial activity of ZEC nanocomposite shows the highest in both bacterial strains. These were due to the interaction of the released smaller Ce^{4+} ions that can adhere to the bacterial wall and affects the biochemical process occurring in the cell and cause membrane damage, which leads to cell death. The measured zone of inhabitation against the *E. coli* and *B. subtilis* bacteria was 23 and 21 mm, respectively, which was the highest result from the compared work [65]. Abhilash et al. [66] synthesized Cu_2O, Fe_2O_3, and Fe_2O_3/Cu_2O through the hydrothermal synthesis method and further tested their potential to inhibit bacterial pathogens by the disk diffusion method. Antibacterial activity results demonstrated that a sizable ZOI occurs against test pathogens. Their result showed that among the test samples, Fe_2O_3/Cu_2O composites showed the highest antibacterial activity due to their large surface area. The observed maximum inhibition zones of the nanocomposite were 20.13,

21.09, 08.23, and 20.60 for *S. aureus*, *P. aeruginosa*, *B. subtilis*, and *E. coli*, respectively. In the case of *B. subtilis*, at the same time, only a slight response to Fe_2O_3/Cu_2O nanocomposite was observed. Generally, they concluded that Fe_2O_3/Cu_2O nanocomposite inhibits bacterial pathogens by rupturing the outer and inner cell walls of the bacteria that lead to disorganization and leakage of the cell membrane [66]. Ying et al. [67] synthesized WO_3/ZnO hybrid particles by depositing WO_3 on presynthesized ZnO particles via the liquid impregnation method. They tested the antibacterial activity of this nanocomposite against *B. subtilis*, *S. aureus*, *E. coli*, and *P. aeruginosa* bacterial pathogens. The antibacterial susceptibility assay demonstrated that the presence of WO_3, even at the minimum amount, suppressed the antibacterial activity of ZnO particles, which exhibited a better inhibition effect against gram-positive bacteria than Gram-negative bacteria [67]. Gasmalla et al. [68] investigated the application of Fe_3O_4/Ag_3PO_4/WO_3 as antibacterial properties. *S. aureus* was chosen as a representative microorganism. From their finding, it was presumed that successful deposition of Ag_3PO_4 imparted antibacterial functions on the nanocomposites. The antibacterial mechanism of the as-prepared nanocomposite was performed by interfacial contact between the test samples and the agar plate, which should lead to inhibition of the bacterial growth. From the measured zone of inhabitation, Fe_3O_4 and WO_3 did not show antibacterial activity against the chosen bacterial strains. The inhibition zone radius for the synthesized composites is 13, 19, and 17 mm for Ag_3PO_4, Fe_3O_4/Ag_3PO_4, and Fe_3O_4/Ag_3PO_4/WO_3, respectively. From their result, all Ag_3PO_4-based composites had significant bactericidal activity against *S. aureus*. The comparison between Fe_3O_4/Ag_3PO_4/WO_3 and Fe_3O_4/Ag_3PO_4/WO_3 noncomposite shows an inhibition zone of 12 and 17 mm, respectively [68]. Jan et al. [69] synthesized pristine ZnO and ZnO–CuO nanocomposite through a chemical coprecipitation technique. Using agar disk diffusion and timer kill assessment routine, the antibacterial activity of pristine ZnO and ZnO–CuO nanocomposite was tested. The test has performed against Gram-positive methicillin-resistant *S. aureus* bacterium. The pristine ZnO nanostructures show an 8 mm diameter ZOI, and ZnO–CuO nanocomposite suspension has produced a 24 mm diameter ZOI against *S. aureus* that is significantly higher than pristine ZnO nanostructures. The polyoxyethylene result shows that ZnO–CuO nanocomposite had more surface defects than pure ZnO nanostructures. Therefore, they concluded that the presence of a large number of surface defects in ZnO–CuO nanocomposite could trap the electron and transfer to dissolved oxygen, which leads to large amount of ROS production and, hence, result in higher antibacterial activity [69]. Panchal et al. [70] recommended phytoextract-mediated ZnO/MgO nanocomposites for photocatalytic and antibacterial activities. In their work, they synthesized MgO, ZnO NPs, and ZnO/MgO nanocomposites (NCs) from *Ricinus communis* L. plant seedless fruit extract (SFE) through the green synthesis method. In comparison to the pure NPs and NCs, the ZnO/MgO–NCs (1 : 1) exhibited an enhanced antibacterial activity and resulted in a

TABLE 1: Inhibition zone of pure MgO–NPs, ZnO–NPs, and composites of ZnO/MgO (1 : 2, 1 : 1 and 2 : 1) toward *E. coli* and *Klebsiella* bacteria [70].

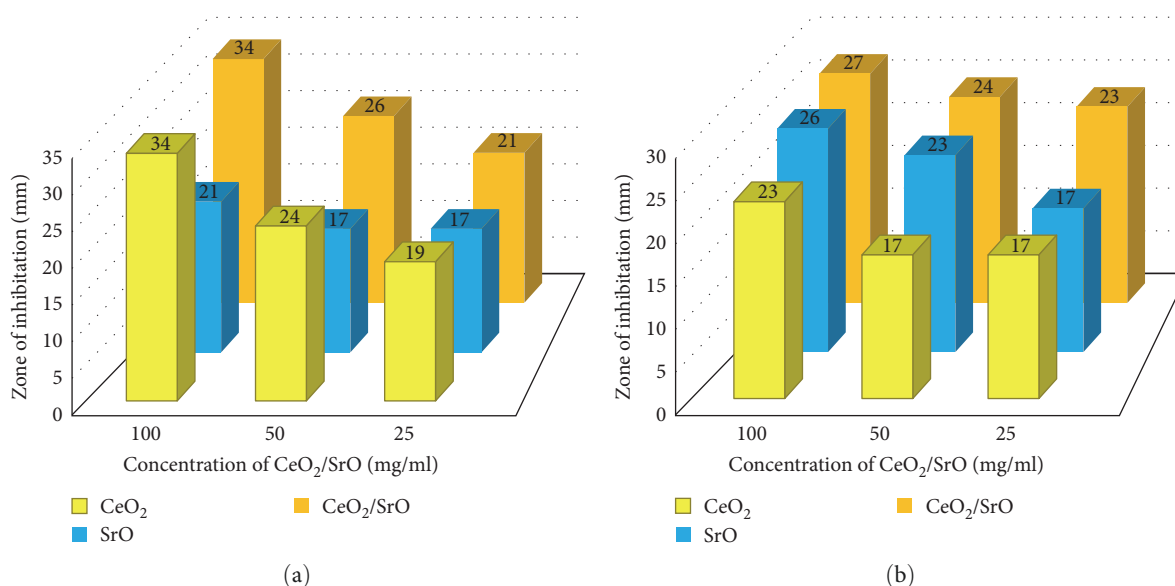| Sr No.	Material	Concentration (mg)	Zone of inhibition (mm) against	
			E. coli	*Klebsiella*
1	Pure MgO–NPs	10	17	14
2	Pure ZnO–NPs	10	10	8
3	ZnO/MgO–NCs (1 : 2)	10	18	15
4	ZnO/MgO–NCs (1 : 1)	10	28	22
5	ZnO/MgO–NCs (2 : 1)	10	14	12

FIGURE 6: (a) Graphical representation of zone of inhibition of mixed metal oxide NCs against Gram-positive bacteria (*S. aureus*); (b) graphical representation of zone of inhibition of mixed metal–oxide NCs against Gram-negative bacteria (*E. coli*) (adapted from [71]).

1.5–2.8 times and 1.27–3.5 times larger radius for the ZOI in the case of *E. coli* and *Klebsiella*, respectively (Table 1) [70].

Pandiyan et al. [71] synthesized SrO/CeO$_2$ nanocomposite with a green synthesis route for antimicrobial activity against *S. aureus* and *E. coli* bacteria with different concentrations of SrO/CeO$_2$. The prepared nanocomposite attacks the bacteria through ROS generation. The lowest bandgap (~3.17 eV), small crystal size, and the nanorod shape of SrO/CeO$_2$ nanocomposite help to have a higher antibacterial activity to the corresponding CeO$_2$ and SrO metal oxides. Figure 6 shows a variation of a ZOI with the concentration of the ceramic mixed metal-oxide nanocomposite [71]. Munawar et al. [72] synthesized triphase ZnO–Yb$_2$O$_3$–Pr$_2$O$_3$ nanocomposite by the coprecipitation method. The grown nanocomposite exhibited superior activity with 26, 29, and 31 ZOI against *S. aureus* and 29, 29, and 30 ZOI against *E. coli* bacterial strains at concentrations of 10, 20, and 40 g/ml. They also compared the antibacterial activity of ZnO–Yb$_2$O$_3$–Pr$_2$O$_3$ nanocomposite with other researchers' work. Their work shows high antibacterial activity than others. They suggested that a small crystallite size and larger surface area of the nanocomposite could cause a high

production rate of ROS species that can cause the destruction of cellular proteins and DNA or may cause the death of the cell, facilitating the mass transportation and diffusion of reactant molecules [72].

Ahmad et al. [73] synthesized ZnO/Ag$_2$O that showed an increment in the zone of inhabitation from 17 to 34 mm in the case of *E. coli* and also for *B. subtilis* from 19 to 30 mm as compared to the inhibition zones of ZnO. This test also proved that the NCs are effective [73]. Kannan et al. [74] used a microwave-assisted synthesis technique to study the antibacterial activity of CdO–CuO nanocomposite. The test had performed against Gram-positive *S. aureus* and Gram-negative *S. typhi* bacterial strains. The antimicrobial property of the nanocomposite at concentrations of 50 and 100 g/ml exhibits higher antibacterial performance against *S. aureus* (26 mm) at a concentration equal to 100 g/ml [74]. In the same year, Syed et al. proposed that CeO$_2$–ZnO extracted from *Acacia nilotica* fruit has good antibacterial activity against *Klebsiella aerogenes* and *S. aureus* bacterial strains. The antibacterial properties of the nanocomposite were performed via the agar WD method for both pathogen strains. The inhibition zones of the bacterial strains measured at
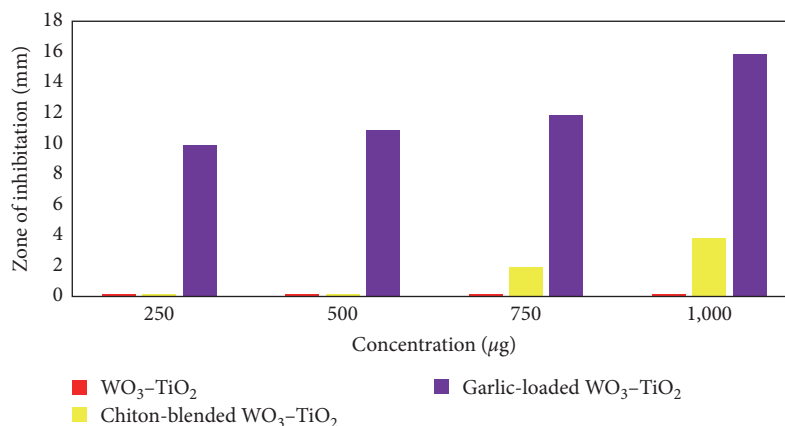
FIGURE 7: Comparable inhibition zone (mm) for WO_3–TiO_2, chitosan blended WO_3–TiO_2, and garlic-loaded WO_3–TiO_2 nanocomposites in an *E. coli* bacterial strain [77].

500 and 1,000 μg concentrations show an increase in antibacterial activity of the nanocomposite with the concentration. The nanocomposite also exhibited better antibacterial performance than pure ZnO and CeO_2 NPs [75]. In this year, Sunaryono et al. successfully synthesized ZnO/TiO_2 nanocomposite by coprecipitation method. Their result shows that the inhabitation zone is greater than the individual nanoparticle, i.e., 7.71 mm for *S. aureus* and 13.40 mm for *E. coli* bacterial pathogens [76]. Dhanalekshmi et al. [77] synthesized novel garlic-loaded WO_3–TiO_2 chitosan (CS)-blended WO_3–TiO_2 and WO_3–TiO_2 nanocomposites by a simple sol–gel and precipitation methods. The antimicrobial activities of WO_3–TiO_2, CS-blended WO_3–TiO_2, and garlic-loaded WO_3–TiO_2 were determined by using a WD method employing Gram-negative bacteria (*E. coli*) with four different concentrations (250, 500, 750, and 1,000 g). The inhibition zones of all nanocomposites are shown in Figure 7. The WO_3–TiO_2 nanocomposite is inert to the antibacterial activity. CS-blended WO_3–TiO_2 has no antibacterial activity for 250 and 500 g but shows significantly less activity for 750 and 1,000 g. Garlic-loaded WO_3–TiO_2 exhibited good antibacterial activity for all four concentrations. Due to the presence of the allicin compound in garlic, the garlic-loaded nanocomposite had a higher inhibitory effect on the growth of *E. coli*.

Allicin compound decomposes into other sulfurous compounds such as diallyl disulfide and ajoene. Sulfurous compounds interact with the cell wall of bacteria by rupturing their layer and changing their total metabolic activity, thereby inhibiting the bacterial activity of the cell [77]. CdO–CuO–ZnO (CCZ NC) mixed metal-oxide nanocomposite was proposed for antibacterial and photocatalytic activities in 2021 by Kannan et al. [74]. The antimicrobial property of the NC was performed against Gram-positive bacteria (*S. aureus*) and Gram-negative bacteria (*S. typhi*) with a concentration of 50 and 100 g/ml. At 100 g/ml, the CCZ NC had higher antibacterial action against *S. aureus* (28 mm) and *S. typhi* (22 mm). The antibacterial mechanism of the fabricated CCZ NC could be elucidated by the manufacture of ROS and the discharge of heavy metal ions [78].

Kannan et al. synthesized NiO–CYO–CSO in the same year by wet chemical route to study the structural, electrochemical, photocatalytic, and antibacterial properties. The antimicrobial test was performed against *Staphylococcus epidermidis*, *E. coli*, and *A. hydrophila* with disruption of cell walls/membranes and generation of ROS to damage membranes of the bacterial cell. By varying the concentration of the composite from 20 to 80 g/ml, they obtained a high ZOI (22, 18, and 22 nm) at 80 g/ml concentration [79]. A rare-earth-based mixed metal-oxide nanocomposite (NiO–CGYO) was proposed by Kannan et al. in 2021 [74]. It shows excellent antibacterial activity against Gram-negative (*Shigella flexneri*, *E. coli*) and Gram-positive (*Micrococcus luteus*, *R. rhodochrous*) bacterial pathogens [80]. Uyen et al. [81] proposed that Cu_2O–ZnO nanocomposite has excellent antimicrobial performance than Ag–ZnO and ZnO NPs when they compared to their work. In this work, they got 0.16 and 1.25 mg/ml MIC for *S. aureus* and *E. coli* bacterial strains that are greater than that of the works mentioned above. They also show that the antibacterial activity of Cu_2O–ZnO nanocomposite was reduced after 45 days when stored at room temperature in a becher without cover [81]. Mukhtar et al. [82] tested the antibacterial features of ternary NiO–Fe_2O_3–CdO and binary NiO–Fe_2O_3–CdO, NiO–CdO nanocomposites. The prepared nanocomposites were tested against *E. coli* bacteria by varying the concentrations (10, 20, 30, and 40 g/ml). They also compared the assessment of the antibacterial activity of NiO–Fe_2O_3–CdO nanocomposite with other research work in which their work shows higher antibacterial activity than others. In addition, their result indicates that ternary nanocomposite shows higher antibacterial activity (17 mm) compared to binary nanocomposite (14 mm) at 40 g/ml concentration. The higher inhibition zone of nanocomposite is due to contact stress or direct oxidation, in addition to the heavy metals Ni^{2+}, Fe^{3+}, and Cd^{2+} ions in the nanocomposite's surface can communally interconnect with the cell membrane, which is negatively charged. These metal ions cause the death of microbes by penetrating the cell membrane [82]. Rahmah et al. [83] used the hydrothermal synthesis
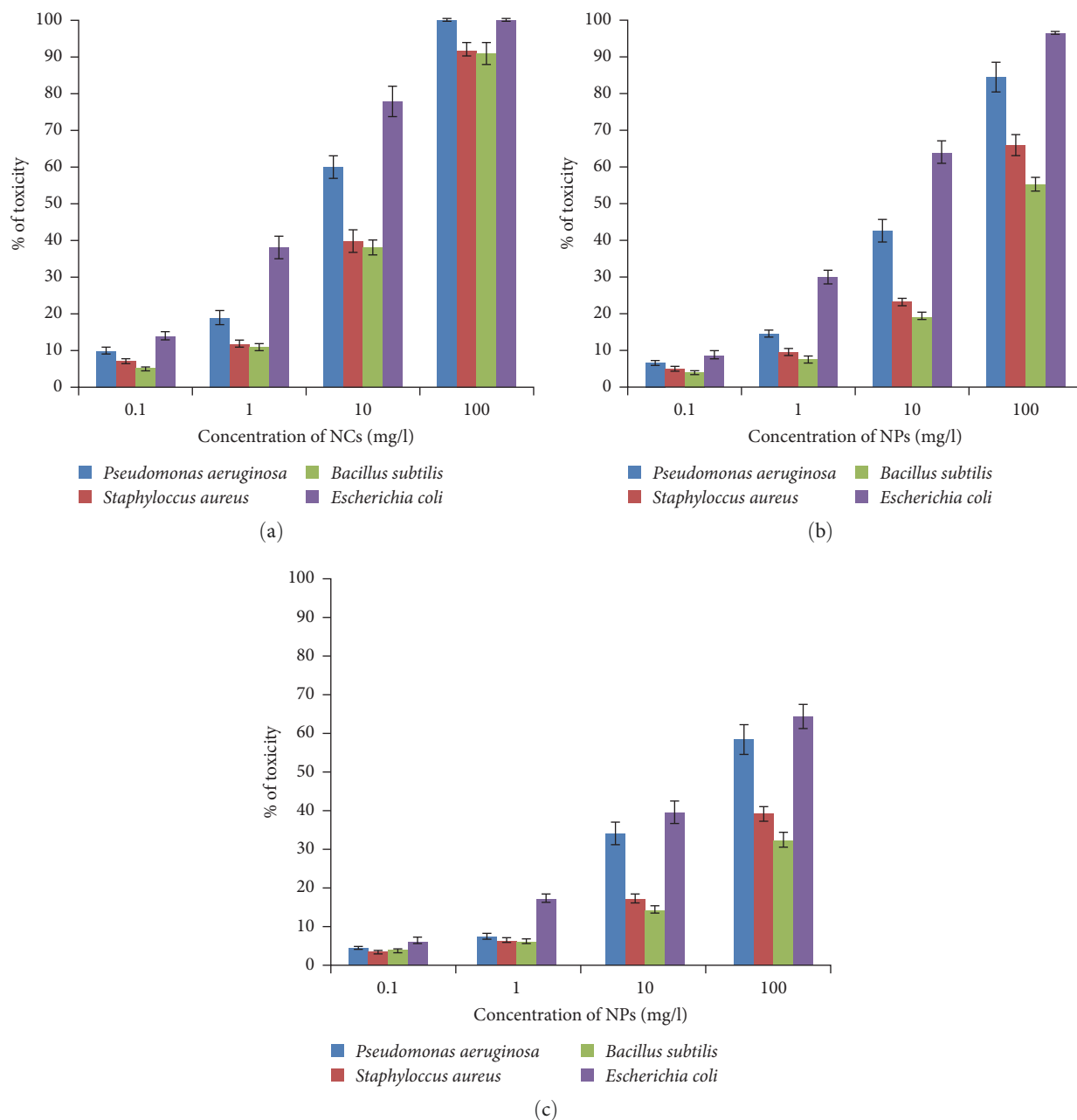
(a)

(b)

(c)

FIGURE 8: The antibacterial effect of (a) CeO_2/Al_2O_3 and (b) CeO_2 and (c) Al_2O_3 on *P. aeruginosa*, *S. aureus*, *B. subtilis*, and *E. coli* [84].

of $\gamma-Fe_2O_3/Ag_2O$ nanocomposite that is used to study their antibacterial activity against Gram-positive bacteria (*S. aureus* and *S. epidermidis*), Gram-negative bacteria (*E. coli* and *K. pneumoniae*), and fungi cultures Gram-positive (*C. albicans*) with a zone of inhabitation (18 and 13 mm) for Gram-positive, 13.5 and 13 mm for Gram-negative, and 13 mm for the cultured fungi. The antibacterial activity of $\gamma-Fe_2O_3/Ag_2O$ nanocomposite is mainly associated with the release of silver ions Ag^+ and iron oxide ions (Fe^{2+} and Fe^{3+}) due to their ability to bind the cell wall of bacteria through electrostatic attraction and reacted with the thiol group of bacterial cell wall and blocked the transport of nutrients through the cell wall and finally the bacterial death [83].

Al Farraj et al. [84] reported that the enhancement of the antimicrobial agent of CeO_2 was the loading of Al_2O_3 NP. Their result shows that the antibacterial effect increases when NPs dosage increases as a result of composite formation. Figure 8 shows the antibacterial activity of the synthesized NPs and NCs against different pathogens at different concentrations [84].

Gandotra et al. [85] reported the morphology-dependent antibacterial activities of Cu_xO/ZnO nanocomposites toward *E. coli*. Aqueous Cu_xO nanostructures are photoreduced on solution-grown ZnO nanorods as part of the fabrication process. Different morphologies of Cu_xO nanostructure are verified using scanning electron microscopy such as
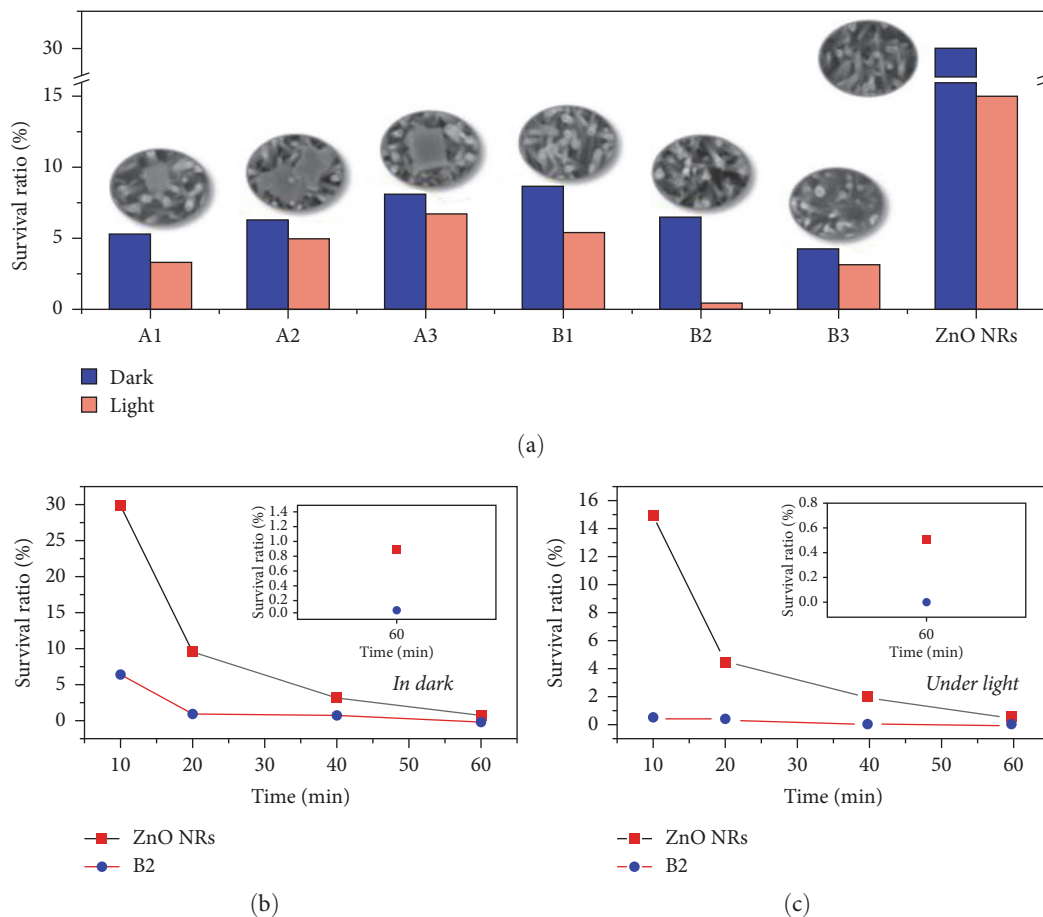
(a)

(b)

(c)

FIGURE 9: (a) Survival ratios for all samples for a 10 min reaction time for A1 (nanocube 1), A2 (nanocube 2), A3 (nanocube 3), B1 (nanoclusture), B2 (nanospike), and B3 (nanoweb). Time-dependent survival ratios for ZnO and B2 (nanospike) (b) in dark and (c) under light. Insets show the ratios at 60 min [85].

nanocubes, nanoclusters, nanospikes, and nanowebs by adjusting the temperature and photoreduction duration. Antibacterial test performed in a dark and under low-intensity blue-light irradiation for a 10 min antibacterial reaction time. The nanoweb sample exhibits the lowest bacterial survival ratio of 4.2% in the dark, and the nanospike sample exhibits the lowest survival ratio of 0.5% under $1 \, \text{mW} \, \text{cm}^{-2}$ blue-light illumination. Furthermore, the nanospike sample and ZnO NRs exhibit remarkable survival ratios of 3×10^{-4} and 10^{-5} in the dark and under light for 60 min, as shown in Figure 9 [85].

Noor et al. [86] synthesized a well-controlled $\text{CeO}_2/\text{CePO}_4$ nanocomposites using *Artocarpus heterophyllus* aqueous leaf extract as a reducing agent. In order to examine cytotoxicity, two mammalian cell lines HeLa and Vero used. Antibacterial activity of synthesized nanocomposite has tested against *S. aureus*, *Bacillus cereus*, *Salmonella typhimurium*, and *E. coli* bacteria. Their study demonstrated that the phytosynthesized $\text{CeO}_2/\text{CePO}_4$ nanocomposites show enhancement in antibacterial efficacy against both Gram-positive and Gram-negative bacteria as compared to the other phytosynthesized CeO_2 nanoparticles found in literature; these might be due to the increase the penetration of positively charged nanocomposites through the negatively

charged bacterial cell walls that result in redox switching between Ce^{3+} and Ce^{4+} in $\text{CeO}_2/\text{CePO}_4$ nanocomposites. The cytotoxicity analyze of $\text{CeO}_2/\text{CePO}_4$ nanocomposites relieved that the cell survival rate was beyond 95%, with a concentration range from 0.5 to 3 g/l [86]. Bisht et al. [87] synthesized bismuth oxybromide (BiOBr) and silver oxide-loaded BiOBr $\text{Ag}_2\text{O/BiOBr}$ nanocomposite using the high efficient solution-based method. Antibacterial activity of the synthesized nanocomposite had tested against five different human pathogens under light and in the absence of light in a concentration ranging from 0.5 to 2.0 mg/ml. Their result showed that $\text{Ag}_2\text{O/BiOBr}$ highly had good antibacterial activity than BiOBr. The MIC of $\text{Ag}_2\text{O/BiOBr}$ was 0.5 mg/ml against *E. coli*, *K. pneumoniae*, and *S. typhimurium*, and 1 mg/ml against *P. aeruginosa* and *Aeromonas salmonicida*, respectively. Minimum bactericidal concentration (MBC) of $\text{Ag}_2\text{O/BiOBr}$ was 1.5 mg/ml against *P. aeruginosa* and *Aeromonas salmonicida*, and 1 mg/ml against *E. coli*, *K. pneumoniae*, and *S. typhimurium* under the observation of light. The result demonstrated that BiOBr and $\text{Ag}_2\text{O/BiOBr}$ have superior bactericidal efficiency and photocatalytic activation in the irradiation with indoor light. $\text{Ag}_2\text{O/BiOBr}$ nanocomposites in the dark show slight inhibition of tested bacterial strains compared to BiOBr. Thus, mere

exposure to indoor light could activate the bactericidal activity of $Ag_2O/BiOBr$ nanocomposites [87].

4.2. Metal-Metal-Oxide Nanocomposites for Antibacterial Activities. This class of nanocomposites is intended to contain both metal and metal oxide. They are further classified into metal ornamented metal-oxide nanoarrays, metal-metal-oxide yolk/shell nanostructures, Janus noble metal/metal-oxide nanostructures, and metal/metal-oxide core/shell nanostructures based on the geometric arrangement [88]. The effectiveness of Ag–ZnO NC on Bacillus thuringiensis, E. coli, and P. aeruginosa was examined by Ghosh et al. [89] by adjusting the concentration of the nanocomposite using a microwave-assisted manufacturing process (i.e., 10, 20, 50, 100, and 200 g). According to the findings, P. aeruginosa, a pathogenic bacterium, formed a negligible inhibition zone with Ag–ZnO NC, although E. coli and B. thuringiensis were sensitive to 200 g NC concentration, generating an inhibition zone of 15 and 9 mm. The antibacterial activity of the greenly produced $Ag@Fe_2O_3$ and Fe_2O_3 NPs was examined by Kulkarni et al. [90] utilizing the agar WD and National Committee for Clinical Laboratory Standards macrodilution broth method. At concentrations of 20, 40, 60, 80, and $100 \mu g \, ml^{-1}$ for both pure Fe_2O_3 and $Ag@Fe_2O_3$ nanocomposites, the produced material's antibacterial activity was evaluated against the bacterium S. aureus and E. coli. At 60 and $40 \mu g \, ml^{-1}$ concentrations of Fe_2O_3 NPs, S. aureus and E. coli exhibit antibacterial action. However, $Ag@Fe_2O_3$ nanocomposite shows excellent growth inhibition at all concentrations, indicating that the addition of Ag has enhanced the antibacterial activity of Fe_2O_3 [90]. Using an Alamar Blue Assay (ABA) absorbance method, Tibayan et al. produced Ag/SnO_2 nanocomposite in 2019 to study the antibacterial capabilities. Their research revealed that the toxicity of E. coli and S. aureus rose with the amount of Ag present in the composite, indicating that the 4 : 1 ratio of Ag to SnO_2 exhibits good antibacterial action. Furthermore, when particle size was decreased from the micro to nanometer range, the antibacterial properties of the composites were improved [91]. Citrus sinensis fruit extract was used as a reducing and stabilizing agent during the green synthesis of a novel $Au@Fe_2O_3$ nanocomposite by Shams et al. [92]. With inhibitory zones of 20($\pm$0.5) mm for E. coli and 20($\pm$0.8) mm for B. subtilis, respectively, the $Au@Fe_2O_3$ nanocomposite demonstrated outstanding antibacterial properties $2 \, mg \, ml^{-1}$ (120 g). A ZOI of 18($\pm$0.4) for E. coli and 15($\pm$0.5) for B. subtilis at $1 \, mg \, ml^{-1}$ (60 g) for the antibacterial activity was also noted. It is evident from the data that $Au@Fe_2O_3$ is more effective against the studied bacterial strains when used at higher concentrations because these bacteria exhibit more microbial activity [92]. Hassanpour et al. [93] used the WD method to determine the antimicrobial activity of Ni/ZnO nanocomposites against 12 bacteria. However, the synthesized composite shows antibacterial activity in the three of them (P. aeruginosa, B. subtilis, and C. albicans) with a diameter inhibition zone of 15, 14, and 9 mm and also 125, 15, and 200 MIC values, respectively [93].

According to the baking duration and S. aureus growth temperature, Muflikhun et al. [94] created Ag/TiO_2 nanocomposite in various forms. Ag/TiO_2 nanocomposite nanorods are the only contender among the several shapes in this study that can destroy bacteria by rupturing their membrane using the sharp point at the top of their shape [94]. Khan et al. [95] created an Ag/Fe_2O_3 nanocomposite using an aqueous extract of Aglaia monozyga leaves. The extracted leaf serves as a natural source for the reduction and stability of the nanocomposite. With ZOI of 23, 21, and 19 mm, respectively, the Ag/Fe_2O_3 nanocomposite strongly inhibits the development of S. aureus, E. coli, and Pseudomonas putida [95]. The usual disk diffusion approach was used by Saranya et al. [96] to conduct bactericidal testing on Ag/Fe_2O_3 NCs. Utilizing A. vera gel extract as a gentle, safe, reusable, and active stabilizer without the use of any hazardous chemicals, Ag/Fe_2O_3 NCs were made using a one-pot microwave-assisted process. As model strains, S. aureus and E. coli, two different bacterial species, were used. The outcome shows that the presence and rising concentration of Ag/Fe_2O_3 NCs indicate a rising inhabitation against all the investigated species. Inhibition diameters for S. aureus were 8.21 ± 0.45, 8.75 ± 0.31, 9.32 ± 0.61 and 11.69 ± 0.63 mm, whereas those for E. coil were 12.13 ± 0.22, 14.36 ± 0.41, 15.01 ± 0.18 and 17.16 ± 0.41 mm. Similar to other researchers, gram-negative E. coli's inhibition rate was substantially higher than that of Gram-positive bacteria (S. aureus). This could be the presence of different bacterial strains with thicker cell walls. Gram-positive bacteria (such as S. aureus) often have a dense cell wall made up of many mucopeptides and lipoteichoic acid surface constituents, whereas Gram-negative bacteria (such as E. coli) have a relatively thin cell wall. As a result, Gram-negative bacteria's cell wall on the membrane has an opportunity to interact with the manufactured Ag/Fe_2O_3 NCs and kill the bacterial cell by entering the bacterial cell, degrading lipopolysaccharide molecules, creating membrane permeability, and resulting in DNA damage [96]. CuO/Ag and ZnO/Ag nanocomposites that are separately made using a mixed wet chemical process were examined for their antibacterial activity by Asamoah et al. [97]. Due to the production of the composite with silver, CuO and ZnO's energy bandgaps have shrunk, according to UVvis spectroscopy analysis. ROS, which are harmful to bacterial cells, are created as a result of the discharge of electrons at a lower energy wavelength than the individual metal oxides. Using Kirby–Bauer disk diffusion and microdilution techniques, the antibacterial activity of nanocomposites is examined against Gram-negative and Gram-positive bacteria. According to the Kirby–Bauer disk diffusion test, CuO/Ag and ZnO/Ag both had a MIC of 0.25 mg/ml against S. aureus and E. coli. Microdilution also revealed that ZnO/Ag achieved 91.7% and 89.3% effectiveness against both bacterial species, as opposed to CuO/Ag's 98.8% and 98.7% efficiency. As shown in the results, S. aureus was more vulnerable to the individual effects of CuO/Ag and ZnO/Ag nanocomposites than E. coli (Figure 10) [97].
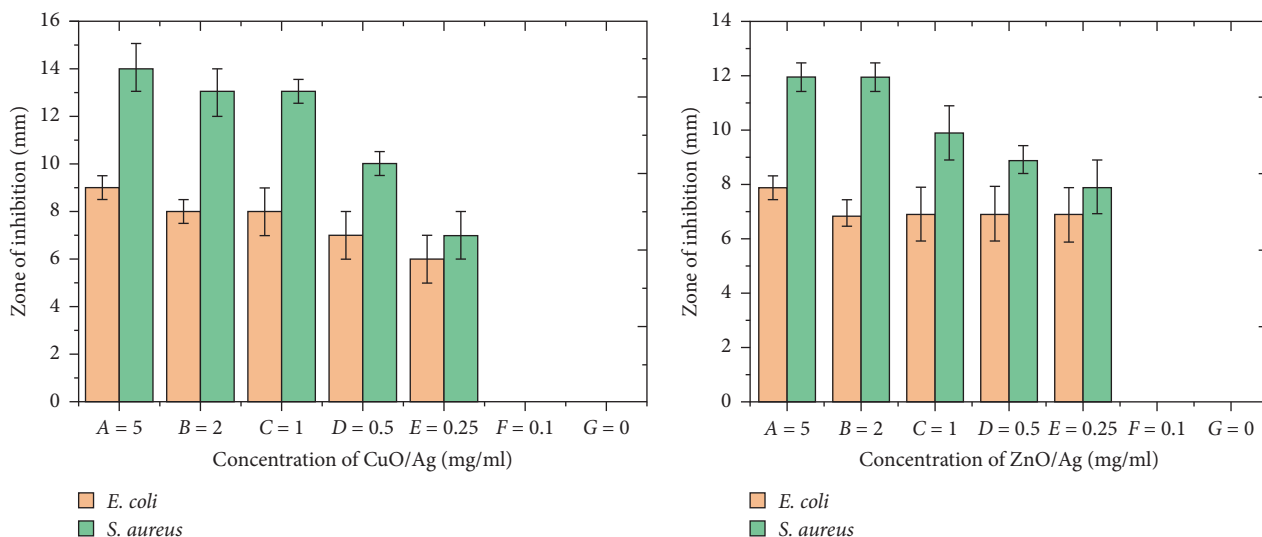
FIGURE 10: The antibacterial activity of CuO/Ag and ZnO/Ag nanocomposite against *E. coli* and *S. aureus* at 5, 2, 1, 0.5, 0.25, 0.1, and 0 mg/ml [97].

In a study by Bhardwaj and Singh (2021), green synthetic *Origanum majorana* leaf extract of Ag/TiO$_2$ NCs and TiO$_2$ NPs was tested for antibacterial activity against pathogens of both Gram-positive *S. aureus* and *B. subtilis* and Gram-negative *E. coli* and *P. aeruginosa* bacteria. For all bacterial strains, the ZOI increases when the concentration of Ag/TiO$_2$NCs and TiO$_2$ NPs rises from 25 to 100 mg/ml. However, their findings indicate that Ag/TiO$_2$ has a larger inhibition zone than TiO$_2$ [98]. Bhavyasree et al. [99] reported the biosynthesis of copper oxide/carbon (CuO/C) nanocomposite via the aqueous decoction of *Ficus religiosa* leaves. *Ficus religiosa* leaves are used as a capping factor, an origin of carbon, and a reducing agent to investigate. They studied the antimicrobial, antioxidant, and adsorption properties of the nanocomposite. By evaluating the ZOI at various concentrations (i.e., from 0.25 to 1 mg/ml), the antibacterial performance of the CuO/C nanocomposites against the bacteria *P. aeruginosa*, *Streptococcus mutans*, *E. coli*, *S. aureus*, and *K. pneumoniae*, as well as the fungus *C. albicans* and *Aspergillus niger* was ascertained. The material exhibits the highest bacterial resistance against *S. aureus* compared to other bacteria. The inhibitory zone for *S. aureus* measures 16 mm in diameter, 14 mm for *E. coli*, and 13 mm for *P. aeruginosa*. With *K. pneumoniae* and *S. mutans*, the material displays a 12 mm inhibitory zone. With the fungus *C. albicans*, the best antibacterial effectiveness is shown. The inhibition area's diameter in this instance is 29 mm. They contended that the nanoscale range of nanocomposites, which might have a high dispersion ability that facilitates strong interaction with the microbial surface and OH radicals present in the nanocomposite to bond with the DNA, is responsible for the nanocomposites' maximum antibacterial activity. After that, the distributed nanocomposite enters the microbial cell membrane and modifies the metabolic reaction taking place there, killing the microbes [99].

5. Polymer–Metal-Oxide Nanocomposite for Antibacterial Activities

Polymer nanocomposites are polymers reinforced with nanomaterials as nanofillers [100]. Polymer nanocomposites have many applications, especially in the automotive and packaging industries. Another highly potential application of polymer nanocomposites is for energy, which includes energy generation and energy storage [101]. To control or restrict the growth of microorganisms and avoid foodborne illnesses and nosocomial infections, the creation of polymer nanocomposites with antimicrobial characteristics is crucial. Antimicrobial polymer nanocomposites are gaining an ever-increasing interest as promising candidates for healthcare and packaging materials as they can hinder the colonization and transmission of pathogens [102]. Sanmugam et al. [103] proposed novel CS, CS–ZnO, and CS–ZnO–graphene oxide (GO) hybrid composites prepared using a one-pot chemical strategy for dye adsorption characteristics and antibacterial activity. The prepared CS and the hybrids such as CS–ZnO and CS–ZnO–GO are tested for antibacterial studies against *S. aureus* and *E. coli* at different concentrations (0.1, 0.3, 0.5, 0.8, and 1.0 μg/ml) and the manifest inhibition zones measured in the agar plates after incubation. The composite sample has superior antibacterial effects as they were able to kill *S. aureus* and *E. coli*, which are the most resistant and responsible for infections in wounds and contamination of foodstuffs. In general, their result shows that CS–ZnO–GO and CS–ZnO inhibit bacterial growth at lower concentrations than CS [103]. Gutha et al. [104] aimed to design CS/poly(vinyl alcohol)/zinc oxide (CS/PVA/ZnO) beads as a novel antibacterial agent with wound healing properties. The antibacterial activity of CS, CS/PVA, and CS/PVA/ZnO is examined by measuring the diameter of the ZOI. The results show the antibacterial activity was improved when it became a composite form. That is, for *E. coli*, the diameter
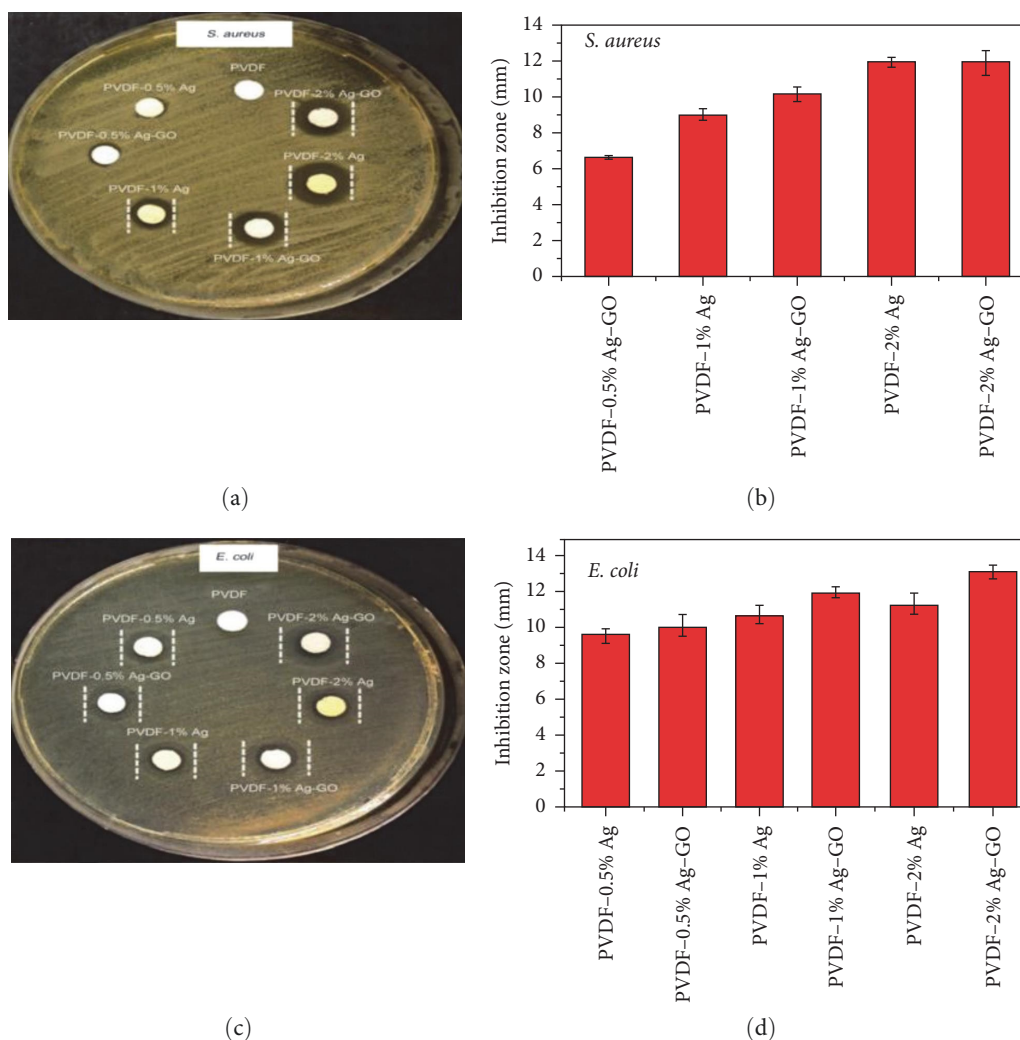
(a)

(b)

(c)

(d)

FIGURE 11: (a) Photograph of *E. coli*; (b) zone of inhibition of electrospun PVDF and its nanocomposite membranes exposed to *E. coli*; (c) photograph of *S. aureus*; (d) zone of inhibition of electrospun PVDF and its nanocomposite membranes exposed to *S. aureus* [105].

of the ZOI was 10 mm in the CS group, 14 mm in CS/PVA group, and 19 mm in CS/PVA/ZnO group. Similarly, the diameter of the ZOI for *S. aureus* was 12 mm in the CS group, 15 mm in CS/PVA group, and 20 mm in CS/PVA/ZnO group. This shows that the mixed CS with another polymer (PVA) and inorganic metal NPs (ZnO) have been introduced into the CS/PVA to improve its antibacterial activity; this is due to the positive charge, which helps (CS and ZnO) to bind the negatively charged cell surface through electrostatic interaction. The incorporation of metal ions and a significant amount of hydroxide group, combined with the biocompatibility and nontoxic properties of PVA, enables an ionic interaction with the negatively charged components of the bacterial cell membrane to be facilitated. This leads to higher antibacterial activity in the synthesized nanocomposite than in the individual components [104]. In 2018, Liu et al. created unique virgin polyvinylidene fluoride (PVDF), PVDF-(0.5%–2%) Ag, and PVDF-(0.5%–2%) Ag-1% GO nanocomposite materials using the electrospinning synthesis method. Generally, all PVDF phases have no antibacterial activity due to the hydrophobic PVDF membrane

that favors the bacteria to adhere to its surface. As we know, bacteria adhere to hydrophobic polymer membranes through hydrophobic–hydrophobic interactions between their cell walls and the membrane surface. Therefore, the antifouling behavior depends on the addition of antibacterial nanofillers such as silver or GO that can inhabit bacteria by releasing Ag^+ ions and attaching to the membrane surfaces. Pure PVDF membrane exhibits a poor or no bactericidal effect against *E. coli*. As shown in Figure 11, the inhibition zone can be readily observed when PVDF is combined with Ag and GO. Therefore, it can be concluded that the antibacterial activity of the PVDF–Ag and PVDF–Ag–GO systems is dependent on the release of Ag^+ ions from the membranes. Furthermore, the incorporation of GO into the PVDF–Ag system also prevents bacteria from attaching to the membrane surface. Finally, PVDF-based nanocomposite membranes have a weaker bactericidal activity for Gram-positive *S. aureus* than Gram-negative *E. coli* because of the difference in the cell wall structure between *S. aureus* and *E. coli* [105]. Beiranvand et al. [106] synthesized hydroxyapatite (HAP), GO, rGO/HAP, $AgNO_3$, and a novel ternary nanocomposite
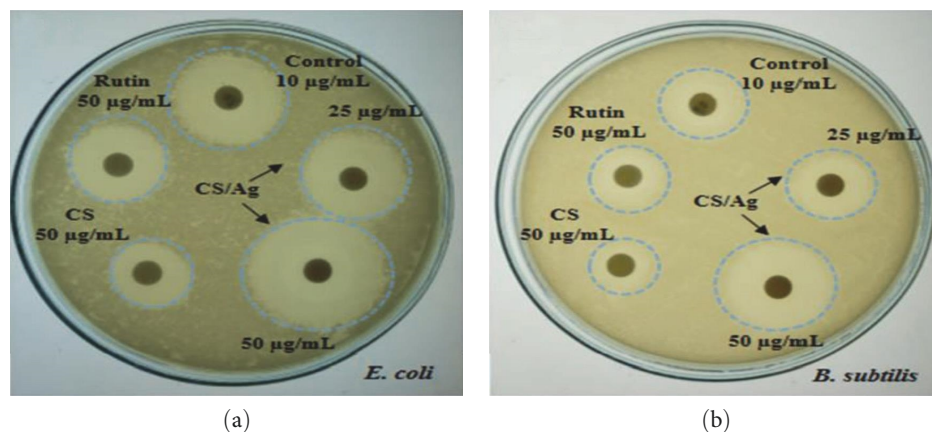
(a)   (b)

Figure 12: Disk diffusion antibacterial activity of CS/Ag nanocomposite (25 and 50 μg/ml), chitosan (50 μg/ml), rutin (50 μg/ml), and control (10 μg/ml) against (a) E. coli and (b) S. aureus [109].

GO/hydroxyapatite/silver (rGO/HAP/Ag) by a simple hydrothermal method. The antibacterial activity of the prepared NP and nanocomposite was tested by the disk diffusion method against Gram-positive and Gram-negative bacterial strains. From the investigated result, the prepared sample of HAP, GO, and rGO/HAP did not show bactericidal activity against bacterial strains. According to these results, Ag NPs play a determinant role in the antibacterial effect in the ternary rGO/HAP/Ag nanocomposite. Its broad-spectrum antibacterial activities at low concentrations, safety in usage, good biocompatibility, intrinsic stability, and low solubility in aqueous media make Ag a good candidate for antibacterial activity.

The average inhibition zones for the antibacterial activity of the rGO/HAP/Ag nanocomposite at the concentration of 35 μg/ml against the given bacteria strains were 28 mm for Bacillus cereus, 30 mm for S. aureus, 5 mm for E. coli, and 7 mm for K. pneumoniae, respectively [106]. Bharathi et al. [107] reported that CS–ZnO nanocomposite showed significant antibacterial activity against chosen bacterial pathogens. Disk diffusion antibacterial activity assessment method is used for different concentrations of nanocomposite and rutin. The prepared nanocomposite shows an excellent antibacterial activity compared to control and bioflavonoid rutin. The recorded zone of inhibition are 25.5 ± 0.50 mm for E. coli, 24.5 ± 0.50 mm for K. pneumoniae, S. aureus (22.5 ± 0.50 mm), and B. subtilis (21 ± 0.50 mm) at 40 μg/ml concentration of the nanocomposite. In addition, the bioflavonoid rutin did not exhibit any zone of inhibition in the chosen pathogens [107]. Dejen et al. [108] successfully synthesized ZnO/PVA NCs using the solution casting method. ZnO/PVA NCs extracted from an aqueous Moringa oleifera leaf in various ratios of precursor salt, and ZnO-coated PVA nanocomposites from 5%, 9%, 13%, and 16% by wt of ZnO and PVA. The antibacterial activity of the synthesized ZnO and ZnO/PVA NCs was evaluated against E. coli and S. aureus bacteria. Based on the obtained result, the antibacterial activity of PVA is not much significant compared with ZnO NPs, which revealed that the antibacterial activity of the tested composite sample is dependent on the concentration of ZnO NPs in the polymer matrix. The antibacterial

inhibition efficiency of ZnO/PVA NCs is increased with the concentration of ZnO from 5.5 to 17 mm on average for E. coli and from 5.5 to 22.2 mm on average for S. aureus at 16% activity concentration [108]. Nandana et al. [109] studied the bactericidal activity of synthesized CS/Ag nanocomposite, evaluated by the agar disk diffusion method against B. subtilis and E. coli. The synthesized CS/Ag nanocomposite showed significant antibacterial activity against tested bacterial pathogens. The measured zone of inhibition for CS/Ag nanocomposite against tested pathogens are as follows: 13 mm for 25 μg/ml and 19 mm for 50 μg/ml and 11 mm of ZOI for 25 μg/ml, and 14 mm for 50 μg/ml against E. coli and B. subtilis, respectively. As shown in Figure 12, the synthesized nanocomposite has excellent antibacterial activity than the rutin and CS. The rutin exhibited potential activity, whereas CS showed moderate antibacterial activity against the tested bacterial pathogens [109].

6. Other Nanocomposites for Antibacterial Activities

Jana et al. [110] studied the antibacterial activity of CdS/ZnO nanocomposites using the WD agar method with a concentration ratio of CZ1 : 1, CZ1 : 2, and CZ1 : 3 without light irradiation. Their result showed all the prepared samples have an antibacterial effect against the selected bacterial strains without light irradiation. But, the CdS/ZnO composite with a 1 : 3 ratio shows the highest antibacterial activity against E. coli, S. aureus, and K. pneumoniae with a zone of inhabitation of 14, 22, and 13 mm, respectively, in contrast to CZ1 : 1 and CZ1 : 2 samples. They also tested the antibacterial activity of bare CdS and ZnO that did not show antibacterial activity without light irradiation. The inhibition zone against all bacteria increases with the nanocomposite containing a higher ZnO component. This result indicates that the amount of ZnO in the nanocomposite affects the antibacterial activity of the sample against the bacterial strains [110]. Archana et al. [111] synthesized GO–zinc oxide (GO–ZnO) nanocomposite by a simple hydrothermal method. The GO–ZnO composite NP was subjected to
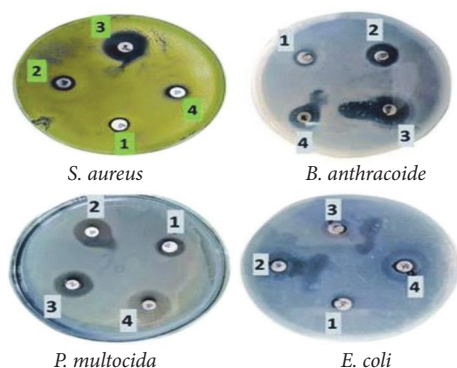
FIGURE 13: Effect of Ag (1), GO–Ag (2), GO–TiO$_2$@ZnO (3), and GO–Ag–TiO$_2$@ZnO (4) on Gram-positive and Gram-negative bacteria [112].

antimicrobial activity through the disk diffusion method, and the MIC was measured by the dilution method. The nanocomposite demonstrated in vitro antimicrobial activity against the four bacterial strains *S. aureus*, *B. subtilis*, *E. coli*, and *P. aeruginosa*, and two strains of fungi, namely, *Aspergilus flavus*, *C. albicans*. The result of the antimicrobial activity increases as the concentration of GO–ZnO nanocomposites increases. The antibacterial properties of GO–ZnO composites are mainly attributed to adhesion with bacteria because of their opposite electric charges resulting in a reduction in the bacterial cell wall [111]. El-Shafai et al. [112] examined the antibacterial activity of novel nanocomposites-based GO nanosheet decorated by silver, titanium dioxide, and zinc oxide nanoflower. Different properties of ZnO, Ag, and GO motivate them to synthesize GO–Ag–TiO$_2$@ZnO nanocomposite. Ag ions have a strong oxidation activity and superhydrophilicity that cause membrane damage and disturb DNA replication of the bacterial cell. ZnO shows antibacterial activity by producing ROS and/or accumulating NPs in the cytoplasm that causes the interruption and suppression of membrane and cellular functions, and GO has a sharp edge that can harm the bacterial cell membrane. The fabricated GO–Ag, GO–TiO$_2$@ZnO, and GO–Ag–TiO$_2$@ZnO (0.005 g/10 ml water) nanocomposites were used to investigate antibacterial activity against Gram-positive bacteria (*S. aureus* and *B. anthracoid*) and Gram-negative bacteria (*E. coli* and *Pasteurella multocida*) by using the disk diffusion method. Their result reveals that all nanocomposites were potentially effective in suppressing bacterial growth with variable potency. The GO–TiO$_2$@ZnO nanocomposite exhibits strong antimicrobial activity against both bacterial species. All of the examined microorganisms were least inhibited by Ag NPs alone. The overall results revealed that these nanocomposites are more effective against Gram-negative than Gram-positive bacteria, as shown in Figure 13 [112].

Bhavyasree et al. [113] are the first researchers that develop copper oxide/carbon (CuO/C) nanocomposites by green synthesis. *Adhatoda vasica* leaf extract is used as a capping agent, reducing agent, and carbon source. The composites were examined for antifungal and antibacterial

activities. They show significant antibacterial activity against the pathogenic bacterial strains *E. coli*, *P. aeruginosa*, *K. pneumoniae*, and *S. aureus* and antifungal activity against the fungi *A. niger* and *C. albicans*. The antibacterial and antifungal activities of the prepared nanocomposite were analyzed by varying the concentration of the composite from 0.25 to 1 mg/ml. The highest antimicrobial activity was observed at 1 mg/ml concentration with a zone of inhabitation 11, 12, 14, and 11 against *E. coli*, *P. aeruginosa*, *K. pneumoniae*, and *S. aureus* and 13 and 14 for *A. niger* and *C. albicans*, respectively. They also predict that the inhibition growth may be due to the interruptions of cell membranes by the nanocomposites resulting in the breakdown of cell enzymes [113]. Sharma et al. [114] synthesized cerium oxide (CeO$_2$) GO nanocomposite that shows good antimicrobial properties against wound pathogens. As a result of the aggregation of CeO$_2$ particles on GO, ROS are generated and inhibited microbial growth. In their work, they examined the antibacterial activity of GO, CeO$_2$ NPs, and CeO$_2$/GO nanocomposite under light and in the absence of light. Their result showed that the prepared NPs and nanocomposites show better antibacterial activity under a light. Figures 14 and 15 show the zone of inhabitation of the prepared NP and NC in the presence and absence of light [114]. Warsi et al. [115] proposed WO$_3$, MXene, and the WO$_3$/MXene nanocomposite as antimicrobial agents. The test was performed through the disk diffusion method against Gram-positive (*S. aureus*) and Gram-negative (*E. coli*, *K. pneumonia*, and *P. vulgaris)* bacterial strains. Due to the structural difference between the cell membrane and cell wall, the as-synthesized sample exhibited different sensitivity levels toward the positive and negative gram strains. All the prepared samples show good antibacterial activity against *S. aureus* as the concentration of the sample increase. All compounds were effective against *K. pneumoniae* in the event of negative bacteria, and the WO$_3$/MXene composite shows strong action at low concentrations. While WO$_3$ and MXene displayed good antibacterial activity that improved with concentration, the WO$_3$/MXene nanocomposite showed no action against *E. coli* and *P. vulgaris*. The reason behind the low or zero antibacterial activity of the WO$_3$/MXene composite against Gram-negative bacterial strains is the presence of an extra outer membrane that increased the resistance to WO$_3$/MXene. Due to its size and agglomeration, antibacterial activity of WO$_3$/MXene nanocomposite decreases with increased concentration. The above two factors make WO$_3$/MXene less toxic and unable to penetrate the bacterial cell wall. On the other hand, the pristine WO$_3$ and MXene showed an increase in antibacterial activity on increasing concentration [115].

7. Factor Affecting the Antimicrobial Activity of Nanocomposite

Antibiotics work by limiting or killing microorganisms in a bacteriostatic or bactericidal manner. These medications interact with any components necessary for microbial metabolism, stopping infections from producing useful
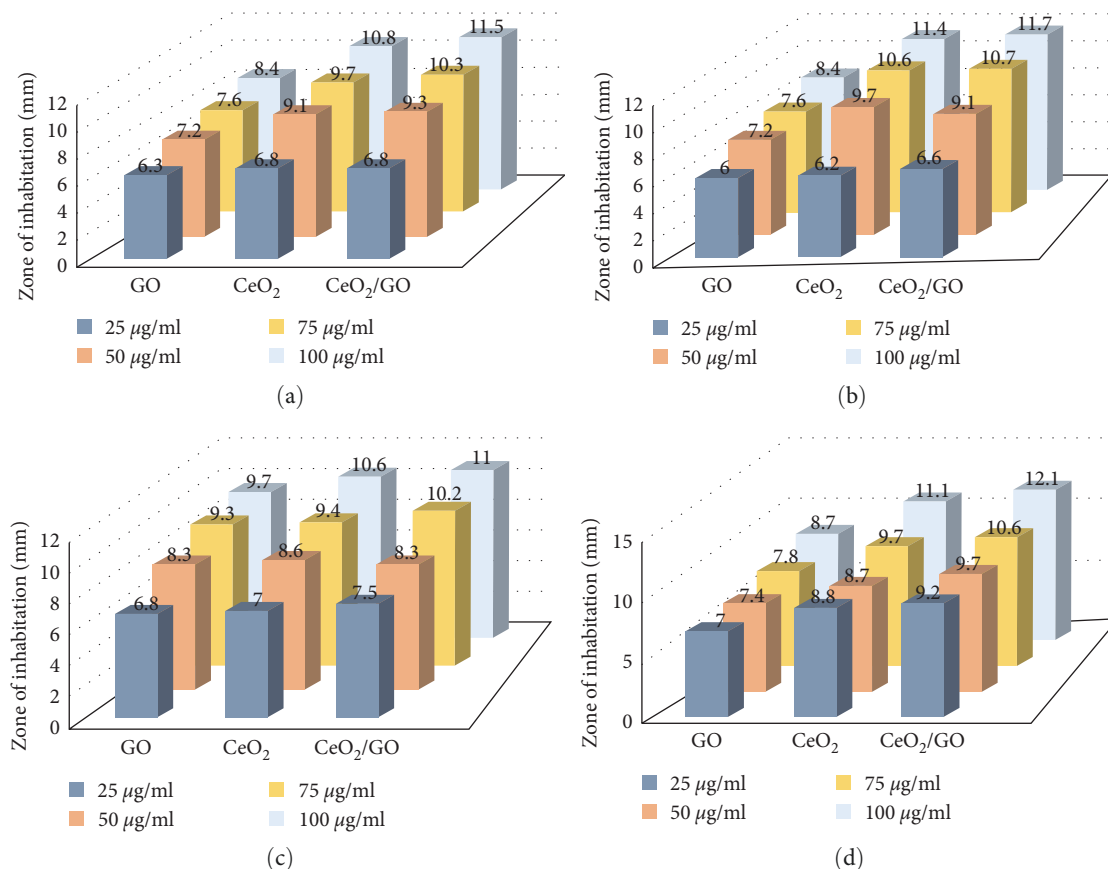
FIGURE 14: Antibacterial activity of GO, CeO$_2$, and CeO$_2$/GO nanocomposites: (a) *Escherichia coli*; (b) *Pseudomonas aeruginosa*; (c) *S. aureus*; and (d) *S. typhi* in the presence of light (adapted from [114]).

biological molecules [116]. Since bacteria may now adapt to medications, treating microbial infections has recently become more difficult; this is why, nanomaterials were developed. The surface area, shape, bacterial type, and material concentration all play major roles in how effectively the nanostructures stop bacterial development by directly contacting their cell walls [88].

7.1. Bacterial Cell Wall. It is crucial to first pay attention to the bacterial cell structure in order to comprehend the mechanisms governing the actions of metal ions, NPs, and nanocomposites. Bacteria are shielded from their frequently hostile environment by a thick, strong, slightly elastic, and multilayered mesh-like structure called a cell wall. This structure also allows for the import and outflow of certain nutrients and cellular waste products. It has a high capacity to determine the antigenicity of bacteria, preserve the morphology of bacteria, shield bacteria from the low-permeability environment, and serve as a potential defense against dangerous substances for bacteria. It is mostly made up of proteins, lipids, and carbohydrates. The bacterium cell wall can be split into two main groups: Gram positive and Gram negative, depending on their structure, components, and functions [1, 117, 118]. Gram staining results in the dark blue or violet coloring of Gram-positive bacteria;

Gram-negative bacteria are unable to retain the stain and instead take up the counterstain, which causes them to appear red or pink [119]. Cell walls, membranes, and cytoplasm make up bacterial cells. Both the preservation of cellular architecture and the maintenance of osmotic equilibrium inside the cytoplasm are functions of the cell wall. The peptidoglycan layer, which is both mechanically and chemically robust and protects the bacterial cell, is typically found outside the cell membrane of the cell wall [120]. Based on the outside of the bacterium, Gram-positive and Gram-negative bacteria differ from one another. Gram-positive bacteria have thicker cell walls with several layers that range in thickness from 20 to 80 nm and are made up of peptidoglycan and teichoic acid, while between the outer cell membrane and the inner plasma membrane of Gram-negative bacteria is a thin layer of peptidoglycan measuring 7–8 nm in thickness. These are what differentiate Gram-positive and Gram-negative responses to an antibiotic. Due to the impenetrable lipid layer in their outer membrane, Gram-negative bacteria are more resistant to antibiotics than Gram-positive bacteria [121]. However, it has been noted that when it comes to NPs with antibacterial characteristics, Gram-positive bacteria exhibit more resistance than Gram-negative bacteria. Two factors account for this: (1) the absence of a thick peptidoglycan coating makes
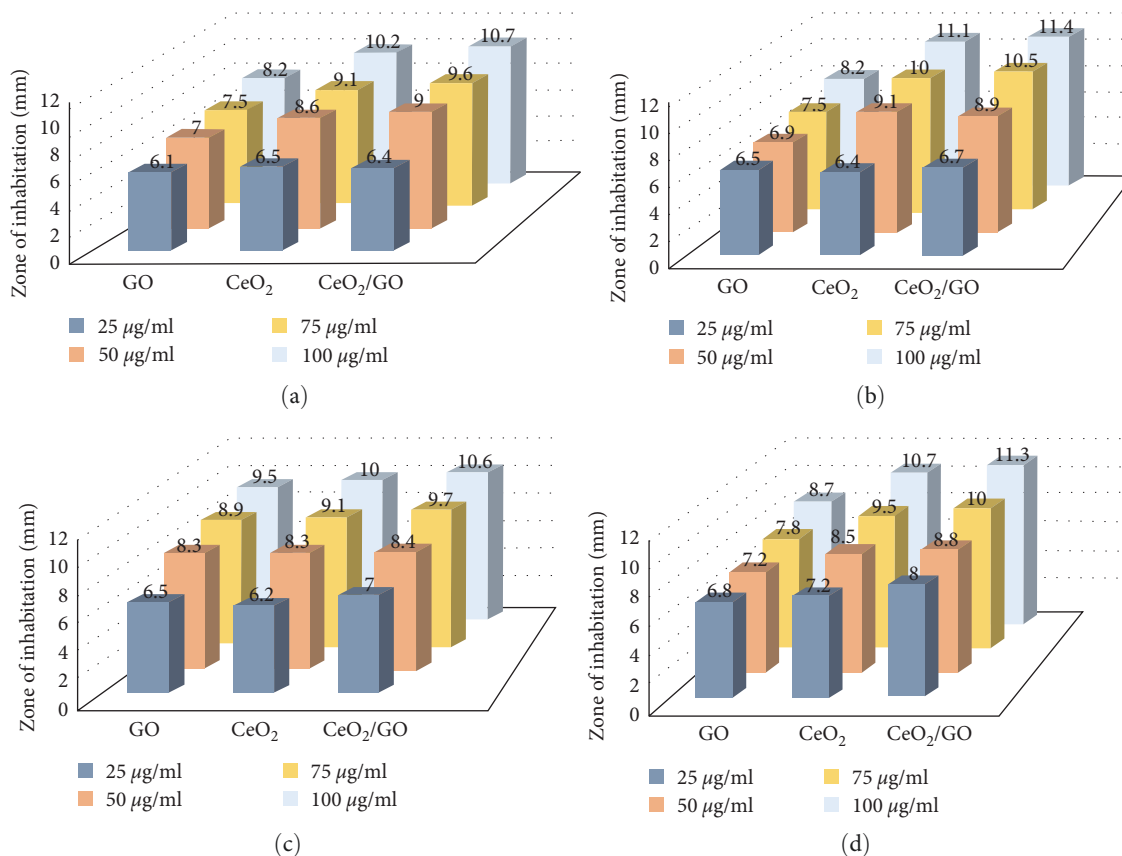
FIGURE 15: Antibacterial activity of GO, CeO$_2$, and CeO$_2$/GO nanocomposites: (a) *Escherichia coli*; (b) *Pseudomonas aeruginosa*; (c) *Staphylococcus aureus*; and (d) *S. typhi* in the absence of light (adapted from [114]).
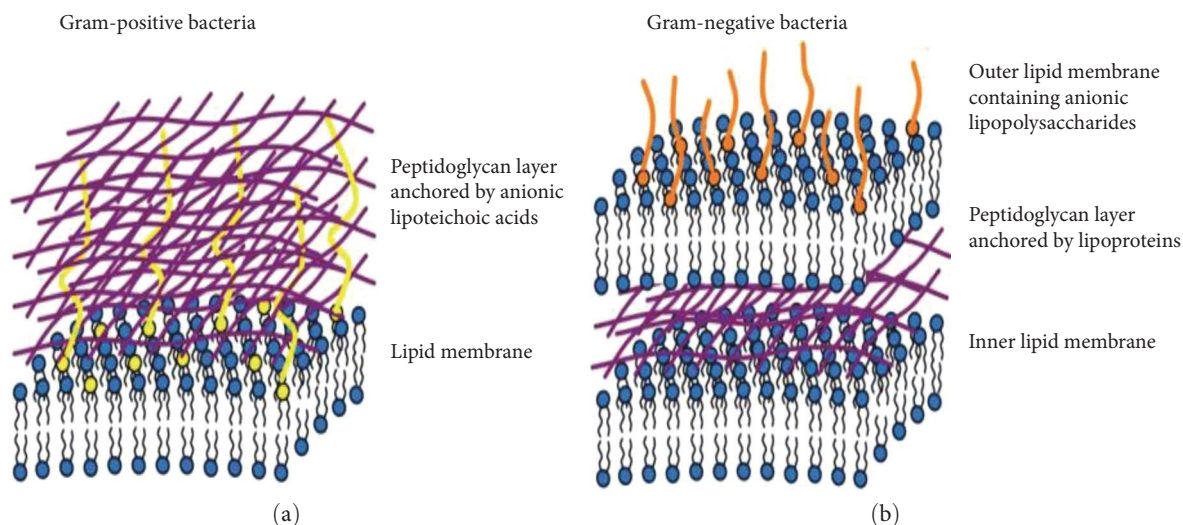

FIGURE 16: Schematic representation showing differences in membrane structures of Gram-positive and Gram-negative bacteria [122].

Gram-negative bacteria more vulnerable; (2) the additional lipopolysaccharide layer increases the amount of time that the bacterial cell membrane is in direct contact with the NPs. This is due to the negative charge of lipopolysaccharide and the positive charge of the majority of NPs, which create attractive forces that promote metal ion uptake and

are detrimental to the bacterial cell [122]. Figure 16 shows the structural difference between Gram-positive and Gram-negative bacterial cell walls.

7.2. Concentration of the Nanocomposite. The concentration of the given composite is the other factor that can affect the
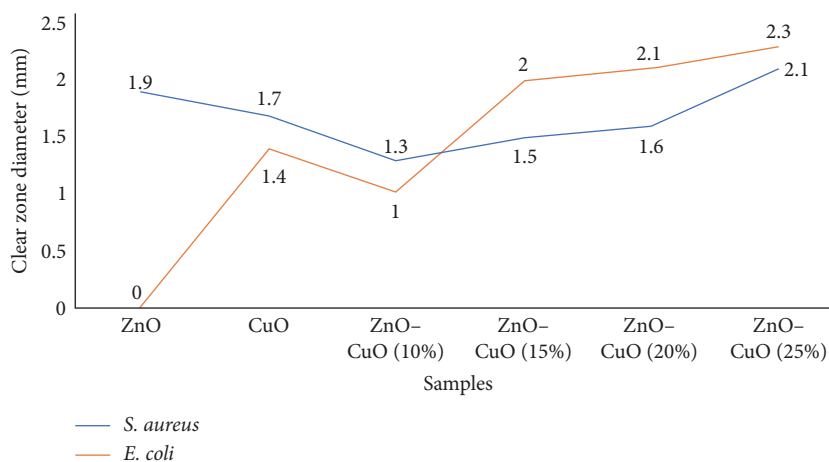
FIGURE 17: The diameter clear zone antibacterial of ZnO, CuO, and CuO–ZnO composites against *S. aureus* and *E. coli* (adapted from [123]).

TABLE 2: Effect of varying concentration of compound in a given composite.

Sr. No.	Nanocomposites	Bacterial strains	Varied compound	References
1	Co@AgNp	*E. coli* and *B. subtilis*	AgNp	[125]
2	CuO–ZnO	*S. aureus*, *Salmonella*, *E. coli*, *B. cereus*, and *P. aeruginosa*	CuO	[126]
3	ZnO–CuO	*E. coli* and *S. aureus*	CuO	[61]
4	ZnO–CuO	*S. aureus*	CuO	[69]
5	WO_3/MXene	*S. aureus*	WO_3/MXene	[118]
6	γ–Fe_2O_3/ZnO	*S. aureus* and *E. coli*	ZnO	[127]
7	ZnO–Ag		Ag	[128]
8	Ppy/ZnO/CS	*S. aureus*, *P. aeruginosa*, *E. coli*, and *B. cereus*	ZnO	[129]
9	CS/Ag	*E. coli* and *S. aureus*	CS/Ag	[109]
10	Ag/Fe_2O_3	*E. coli*, *S. aureus*, and *C. albicans*	Ag/Fe_2O_3	[93]
11	NiO–Fe_2O_3	*E. coli*	NiO–Fe_2O_3–CdO	[82]
12	ZnO/Fe_3O_4/rGO	*E. coli* and *S. aureus*	ZnO/Fe_3O_4/rGO	[130]
13	Fe_2O_3/Ag	*S. aureus* and *E. coli*	Fe_2O_3/Ag	[96]
14	Fe_2O_3/NiO	*B. subtilis*, *S. aureus*, *E. coli*, and *S. typhi*	NiO	[131]

antimicrobial activity of the nanocomposite. Widiarti et al. [123] showed the effect of CuO concentration on antibacterial activity of CuO–ZnO nanocomposite against *S. aureus* and *E. coli* bacteria, as shown in Figure 17. Mohammadi-Aloucheh et al. [61] also showed that the antibacterial activity of ZnO/CuO nanocomposites was slightly influenced by the concentration of CuO in the nanocomposite and increased by increasing its concentration.

The variation in concentration of the given composite can also affect the zone of inhabitation (i.e., MIC is defined as the minimum concentration of an antibiotic to inhibit the bacterial growth that can measure susceptibility and resistance) of the studied bacteria. Some of the literature those are dependent on the concentration of the given material is listed in Table 2. Maulidiyah et al. [124] showed as the potency of

Mn–N–TiO_2 composite wall paint as antibacterial activity was conducted under visible light illumination. They carried out a bacterial test quantitatively based on the percentage reduction of bacterial colonies on media. They vary the concentration of Mn–N–TiO_2 composite coated wall paint from 40% to 60% into the wall paint to obtain high antibacterial activity to inhibit the *S. aureus* bacteria. The presence of several bacterial colonies formed above the nutrient agar surface and the Mn–N–TiO_2 concentration variation affected the total bacterial colonies. Based on their result, the Mn–N–TiO_2 concentration of 60% coated wall paint has better activity in inactivating *S. aureus* bacteria under visible illumination, as shown in Figure 18. This is due to Mn–N–TiO_2 initiated OH radical formed that is capable of bacterial reaction. ROS consisting of ·OH and ·O_2^- are
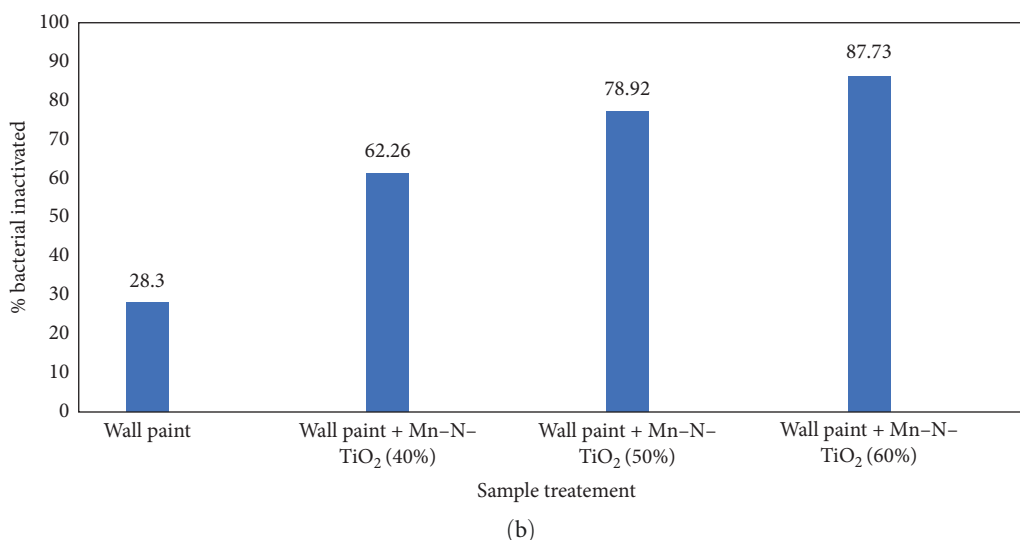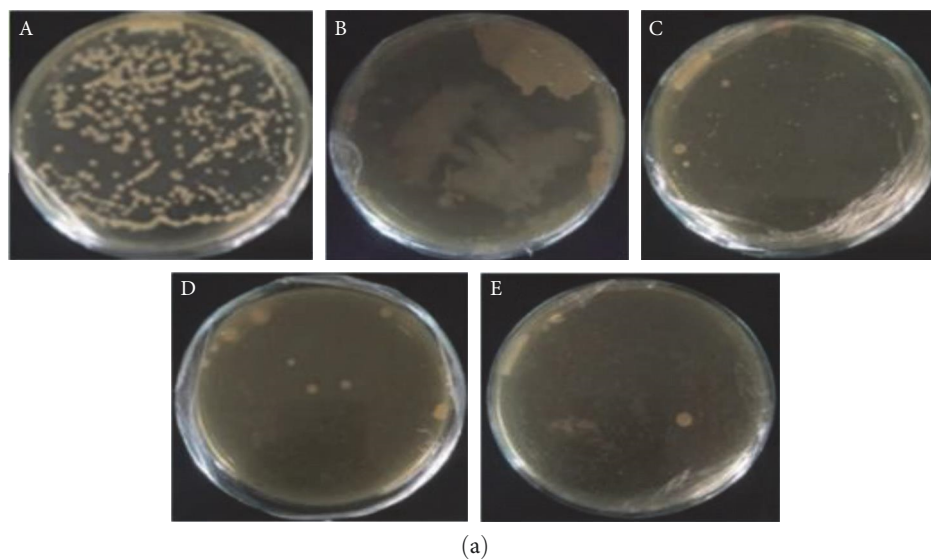
(a)

(b)

FIGURE 18: (a) Photoinactivation of *S. aureus* by variation treatment: (A) without wall paint, (B) wall paint, (C) wall paint coated Mn–N–TiO$_2$ composite (40%), (D) wall paint coated Mn–N–TiO$_2$ composite (50%), and (E) wall paint coated Mn–N–TiO$_2$ composite (60%); (b) percentage of inhibiting *S. aureus* bacteria using Mn–N–TiO$_2$ composite coated wall paint [124].

produced from photogeneration processes on the titania surface by strong oxidative substances to attack cell walls and cell membranes in bacteria [124].

7.3. Energy Bandgap of the Nanocomposite. The bandgap of the synthesized nanocomposite influences antimicrobial activity. The lowest value of the energy bandgap exhibited maximum antimicrobial activities in that electrons are excited from the valance band to the conduction band with small energy. For example, Pandey et al. [132] showed the relationship between the energy bandgap and the antimicrobial activity of ZnO, ZnO–Ag$_2$O/Ag, ZnO–CuO, and ZnO–SnO$_2$ against *P. aeruginosa*, *K. pneumoniae*, *A. baumannii*, and *C. albicans* pathogens. The antimicrobial activity increases as the bandgap of the nanocomposite decreases. Table 3 shows the effect of the bandgap on the antimicrobial activity of selective pathogens.

On the hand, as shown in Table 4, the bandgap of a nanocomposite has an inverse relation to the concentration of the composite material. That is the energy bandgap decreases and have an effective antimicrobial activity as the concentration of the nanocomposite increases.

8. Conclusion and Future Perspectives

In summary, in this review, we see different nanocomposites that are synthesized by different synthesis methods in order to use for antibacterial activity. Nanocomposites are class of materials in which one or more phases with nanoscale dimension (0D, 1D, and 2D) are embedded in metal, ceramic, and polymer matrix. These materials differ from NPs due to their combination, which make them strong and cover the weakness of the individual materials. Recently, NP and nanocomposites materials are more preferable for

TABLE 3: Effect of energy bandgap on the antimicrobial activity of ZnO, ZnO–Ag$_2$O/Ag, ZnO–CuO, and ZnO–SnO$_2$ against different pathogens [132].

Materials	Nanocomposites			
	ZnO	ZnO–CuO	ZnO–SnO$_2$	ZnO–Ag$_2$O/Ag
Energy bandgap	3.25 eV	2.15 eV	3.12 eV	1.98 eV
ZOI for *P. aeruginosa*	8 mm	8.1 mm	7 mm	17 mm
ZIO for *K. pneumoniae*	6.5 mm	8.2 mm	6.25 mm	11.2 mm
ZIO for *A. baumannii*	8 mm	9.25 mm	9 mm	14 mm
ZIO for *C. albicans*	9.5 mm	8 mm	8.5 mm	10.5 mm

TABLE 4: The relation of energy bandgap with particle size, concentration of the nanocomposite, surface area, and zone of inhibition [123].

Sample	Particle size	Bandgap (eV)	Surface area (m^2/g)	Clear zone diameter (mm)	
				S. aureus	*E. coli*
ZnO	26.83	3.39	9.63	1.9	Resistant
CuO	19.83	2.04	21.61	1.7	1.4
10% CuO–ZnO	16.23	2.48	22.48	1.3	1
15% CuO–ZnO	15.56	2.30	22.67	1.5	2
20% CuO–ZnO	16.43	2.23	19.52	1.6	2.1
25% CuO–ZnO	15.74	2.12	28.74	2.1	2.3

antimicrobial activities due to the existence of microorganisms those have resistance to antibiotic. An antimicrobial activity is any chemical or physical compound that can treat, destroy, or prevent the growth of microbes. Due to their nanosized, longer durability, lower toxicity, higher stability, heat resistance, should not react with food or container, have good taste or tasteless, with disagreeable smell and provide mineral elements essential to human cells, nanocomposites are currently used for antibacterial activity. Nanocomposites can inhibit the growth of the bacterial cell by three basic mechanisms, which are releasing metal ions from the surface of the prepared nanocomposite, direct contact to the cell wall of the bacterial, and releasing ROS. The bacterial cell inhabitation mechanism of nanocomposite can be affected by different factors, concentration of the nanocomposite and the bacterial cell wall type are the most common factors that are discussed in this review. However, there are also other factors, which make the antibacterial activity of the nanocomposite in effective like shape and size of the nanocomposite. As we know, the shape and size are the basic physicochemical properties that can directly related to the surface to volume ratio of the given nanoscale materials and have relation on antibacterial mechanism of the nanomaterial. Therefore, we recommended that it is good to study on how the size and shape of the nanocomposite affect the antibacterial activity of a given pathogens.

Data Availability

Data are available on request from the corresponding author.

Conflicts of Interest

The authors declare that they have no conflict of interests.

References

[1] M. J. Hajipour, K. M. Fromm, A. A. Ashkarran et al., "Antibacterial properties of nanoparticles," *Trends in Biotechnology*, vol. 30, no. 10, pp. 499–511, 2012.

[2] H. Van Doan, S. H. Hoseinifar, M. Á. Esteban, M. Dadar, and T. T. N. Thu, "Mushrooms, seaweed, and their derivatives as functional feed additives for aquaculture: an updated view," *Studies in Natural Products Chemistry*, vol. 62, pp. 41–90, 2019.

[3] M. Maruthapandi, A. Saravanan, A. Gupta, J. H. T. Luong, and A. Gedanken, "Antimicrobial activities of conducting polymers and their composites," *Macromol*, vol. 2, no. 1, pp. 78–99, 2022.

[4] A. M. Díez-Pascual and J. A. Luceño-Sánchez, "Antibacterial activity of polymer nanocomposites incorporating graphene and its derivatives: a state of art," *Polymers*, vol. 13, no. 13, p. 2105, 2021.

[5] S. S. Kadri, "Key takeaways from the US CDC's 2019 antibiotic resistance threats report for frontline providers," *Critical Care Medicine*, vol. 48, no. 7, pp. 939–945, 2020.

[6] A. Khezerlou, M. Alizadeh-Sani, M. Azizi-Lalabadi, and A. Ehsani, "Nanoparticles and their antimicrobial properties against pathogens including bacteria, fungi, parasites and viruses," *Microbial Pathogenesis*, vol. 123, pp. 505–526, 2018.

[7] G. Y. Nigussie, G. M. Tesfamariam, B. M. Tegegne et al., "Antibacterial activity of Ag-doped TiO$_2$ and Ag-doped ZnO nanoparticles," *International Journal of Photoenergy*, vol. 2018, Article ID 5927485, 7 pages, 2018.

[8] S. Bayda, M. Adeel, T. Tuccinardi, M. Cordani, and F. Rizzolio, "The history of nanoscience and nanotechnology: from chemical–physical applications to nanomedicine," *Molecules*, vol. 25, no. 1, Article ID 112, 2020.

[9] H. Zheng, R. Ma, M. Gao et al., "Antibacterial applications of graphene oxides: structure-activity relationships, molecular initiating events and biosafety," *Science Bulletin*, vol. 63, no. 2, pp. 133–142, 2018.

[10] A. M. Díez-Pascual, "Antibacterial action of nanoparticle loaded nanocomposites based on graphene and its derivatives: a mini-review," *International Journal of Molecular Sciences*, vol. 21, no. 10, Article ID 3563, 2020.

[11] A. Azam, A. S. Ahmed, M. Oves, M. Khan, and A. Memic, "Size-dependent antimicrobial properties of CuO nanoparticles against Gram-positive and-negative bacterial strains," *International Journal of Nanomedicine*, vol. 7, pp. 3527–3535, 2012.

[12] A. L. Vega-Jiménez, A. R. Vázquez-Olmos, E. Acosta-Gío, and M. A. Álvarez-Pérez, "*In vitro* antimicrobial activity evaluation of metal oxide nanoparticles," in *Nanoemulsions Properties, Fabrications and Applications*, IntechOpen London, UK, 2019.

[13] Y. Jeong, D. W. Lim, and J. Choi, "Assessment of size-dependent antimicrobial and cytotoxic properties of silver nanoparticles," *Advances in Materials Science and Engineering*, vol. 2014, Article ID 763807, 6 pages, 2014.

[14] S. Agnihotri, S. Mukherji, and S. Mukherji, "Size-controlled silver nanoparticles synthesized over the range 5–100 nm using the same protocol and their antibacterial efficacy," *RSC Advances*, vol. 4, no. 8, pp. 3974–3983, 2014.

[15] A. Regiel-Futyra, M. Kus-Liśkiewicz, V. Sebastian et al., "Development of noncytotoxic chitosan–gold nanocomposites as efficient antibacterial materials," *ACS Applied Materials & Interfaces*, vol. 7, no. 2, pp. 1087–1099, 2015.

[16] K. S. Siddiqi, A. ur Rahman, Tajuddin, and A. Husen, "Properties of zinc oxide nanoparticles and their activity against microbes," *Nanoscale Research Letters*, vol. 13, Article ID 141, 2018.

[17] N. Sharma, S. Jandaik, S. Kumar, M. Chitkara, and I. S. Sandhu, "Synthesis, characterization and antimicrobial activity of manganese- and iron-doped zinc oxide nanoparticles," *Journal of Experimental Nanoscience*, vol. 11, no. 1, pp. 54–71, 2016.

[18] S. S. Bandekar, S. N. Hosamane, C. Patil et al., "ZnO-CuO nanocomposites: synthesis, characterization and antibacterial activity," *Journal of Physics: Conference Series*, vol. 1706, Article ID 012018, 2020.

[19] A. Mobed, M. Hasanzadeh, and F. Seidi, "Anti-bacterial activity of gold nanocomposites as a new nanomaterial weapon to combat photogenic agents: recent advances and challenges," *RSC Advances*, vol. 11, no. 55, pp. 34688–34698, 2021.

[20] K. Karthik, S. Dhanuskodi, C. Gobinath, and S. Sivaramakrishnan, "Microwave-assisted synthesis of CdO-ZnO nanocomposite and its antibacterial activity against human pathogens," *Spectrochimica Acta Part A: Molecular and Biomolecular Spectroscopy*, vol. 139, pp. 7–12, 2015.

[21] S. Komarneni, "Feature article. Nanocomposites," *Journal of Materials Chemistry*, vol. 2, no. 12, pp. 1219–1230, 1992.

[22] A. S. Lozhkomoev, O. V. Bakina, A. V. Pervikov, S. O. Kazantsev, and E. A. Glazkova, "Synthesis of CuO–ZnO composite nanoparticles by electrical explosion of wires and their antibacterial activities," *Journal of Materials Science: Materials in Electronics*, vol. 30, pp. 13209–13216, 2019.

[23] A. Bhat, S. Budholiya, S. A. Raj et al., "Review on nanocomposites based on aerospace applications," *Nanotechnology Reviews*, vol. 10, no. 1, pp. 237–253, 2021.

[24] S. Mourdikoudis, R. M. Pallares, and N. T. Thanh, "Characterization techniques for nanoparticles: comparison and complementarity upon studying nanoparticle properties," *Nanoscale*, vol. 10, no. 27, pp. 12871–12934, 2018.

[25] I. Matai, A. Sachdev, P. Dubey, S. U. Kumar, B. Bhushan, and P. Gopinath, "Antibacterial activity and mechanism of Ag–ZnO nanocomposite on *S. aureus* and GFP-expressing antibiotic resistant *E. coli*," *Colloids and Surfaces B: Biointerfaces*, vol. 115, pp. 359–367, 2014.

[26] V. Revathi and K. Karthik, "Microwave assisted CdO–ZnO–MgO nanocomposite and its photocatalytic and antibacterial studies," *Journal of Materials Science: Materials in Electronics*, vol. 29, pp. 18519–18530, 2018.

[27] H. Li, X. Zhou, Y. Huang, B. Liao, L. Cheng, and B. Ren, "Reactive oxygen species in pathogen clearance: the killing mechanisms, the adaption response, and the side effects," *Frontiers in Microbiology*, vol. 11, Article ID 622534, 2021.

[28] J. Bogdan, J. Zarzyńska, and J. Pławińska-Czarnak, "Comparison of infectious agents susceptibility to photocatalytic effects of nanosized titanium and zinc oxides: a practical approach," *Nanoscale Research Letters*, vol. 10, Article ID 309, 2015.

[29] M. Godoy-Gallardo, U. Eckhard, L. M. Delgado et al., "Antibacterial approaches in tissue engineering using metal ions and nanoparticles: from mechanisms to applications," *Bioactive Materials*, vol. 6, no. 12, pp. 4470–4490, 2021.

[30] R. Augustine, A. P. Mathew, and A. Sosnik, "Metal oxide nanoparticles as versatile therapeutic agents modulating cell signaling pathways: linking nanotechnology with molecular medicine," *Applied Materials Today*, vol. 7, pp. 91–103, 2017.

[31] H. Palneedi, J. H. Park, D. Maurya et al., "Laser irradiation of metal oxide films and nanostructures: applications and advances," *Advanced Materials*, vol. 30, no. 14, Article ID 1705148, 2018.

[32] S. R. V. Siva Prasanna, K. Balaji, S. Pandey, and S. Rana, "Metal oxide based nanomaterials and their polymer nanocomposites," in *Nanomaterials and Polymer Nanocomposites*, pp. 123–144, Elsevier, 2019.

[33] S. Stankic, S. Suman, F. Haque, and J. Vidic, "Pure and multi metal oxide nanoparticles: synthesis, antibacterial and cytotoxic properties," *Journal of Nanobiotechnology*, vol. 14, Article ID 73, 2016.

[34] A. Rastogi, M. Zivcak, O. Sytar et al., "Impact of metal and metal oxide nanoparticles on plant: a critical review," *Frontiers in Chemistry*, vol. 5, Article ID 78, 2017.

[35] L. Gnanasekaran, R. Hemamalini, R. Saravanan et al., "Synthesis and characterization of metal oxides (CeO$_2$, CuO, NiO, Mn$_3$O$_4$, SnO$_2$ and ZnO) nanoparticles as photo catalysts for degradation of textile dyes," *Journal of Photochemistry and Photobiology B: Biology*, vol. 173, pp. 43–49, 2017.

[36] A. B. Seabra and N. Durán, "Nanotoxicology of metal oxide nanoparticles," *Metals*, vol. 5, no. 2, pp. 934–975, 2015.

[37] M. S. Chavali and M. P. Nikolova, "Metal oxide nanoparticles and their applications in nanotechnology," *SN Applied Sciences*, vol. 1, Article ID 607, 2019.

[38] A. Lagashetty, S. K. Ganiger, R. K. Preeti, S. Reddy, and M. Pari, "Microwave-assisted green synthesis, characterization and adsorption studies on metal oxide nanoparticles synthesized using *Ficus benghalensis* plant leaf extracts," *New Journal of Chemistry*, vol. 44, no. 33, pp. 14095–14102, 2020.

[39] M. Sharifi-Rad, P. Pohl, F. Epifano, and J. M. Álvarez-Suarez, "Green synthesis of silver nanoparticles using *Astragalus tribuloides* delile. Root extract: characterization, antioxidant, antibacterial, and anti-inflammatory activities," *Nanomaterials*, vol. 10, no. 12, Article ID 2383, 2020.

[40] S. V. Gudkov, D. E. Burmistrov, D. A. Serov, M. B. Rebezov, A. A. Semenova, and A. B. Lisitsyn, "A mini review of antibacterial properties of ZnO nanoparticles," *Frontiers in Physics*, vol. 9, Article ID 641481, 2021.

[41] Y. Li, C. Liao, and S. C. Tjong, "Recent advances in zinc oxide nanostructures with antimicrobial activities," *International Journal of Molecular Sciences*, vol. 21, no. 22, Article ID 8836, 2020.

[42] A. K. Batra, M. D. Aggarwal, M. E. Edwards, and A. Bhalla, "Present status of polymer: ceramic composites for pyroelectric infrared detectors," *Ferroelectrics*, vol. 366, no. 1, pp. 84–121, 2008.

[43] S.-J. Park and M.-K. Seo, *Interface Science and Composites*, vol. 18, Academic Press, Cambridge, MA, 2011.

[44] M. A. Masuelli, "Introduction of fibre-reinforced polymers–polymers and composites: concepts, properties and processes," in *Fiber Reinforced Polymers: The Technology Applied for Concrete Repair*, IntechOpen, 2013.

[45] R. Paul and L. Dai, "Interfacial aspects of carbon composites," *Composite Interfaces*, vol. 25, no. 5-7, pp. 539–605, 2018.

[46] P. Guggilla and A. K. Batra, "Novel electroceramic: polymer composites-preparation, properties and applications," in *Nanocomposites and Polymers with Analytical Methods*, IntechOpen, 2011.

[47] M. Mariano, N. El Kissi, and A. Dufresne, "Cellulose nanocrystals and related nanocomposites: review of some properties and challenges," *Journal of Polymer Science Part B: Polymer Physics*, vol. 52, no. 12, pp. 791–806, 2014.

[48] P. M. Ajayan, L. S. Schadler, and P. V. Braun, Eds., *Nanocomposite Science and Technology*, Wiley-VCH Verlag GmbH & Co. KGaA, 2003.

[49] X. Yan and Z. Guo, "Introduction to nanocomposites," in *Multifunctional Nanocomposites for Energy and Environmental Applications*, pp. 1–5, Wiley-VCH, 1st edition, 2018.

[50] M. Sen, "Nanocomposite materials," in *Nanotechnology and the Environment*, pp. 1–12, IntechOpen, 2020.

[51] N. Pandey, S. K. Shukla, and N. B. Singh, "Water purification by polymer nanocomposites: an overview," *Nanocomposites*, vol. 3, no. 2, pp. 47–66, 2017.

[52] V. Moody and H. L. Needles, "Antimicrobial agents," in *Tufted Carpet*, pp. 145–153, William Andrew Publishing, Norwich, NY, 2004.

[53] M. Balouiri, M. Sadiki, and S. K. Ibnsouda, "Methods for in vitro evaluating antimicrobial activity: a review," *Journal of Pharmaceutical Analysis*, vol. 6, no. 2, pp. 71–79, 2016.

[54] F. Chassagne, T. Samarakoon, G. Porras et al., "A systematic review of plants with antibacterial activities: a taxonomic and phylogenetic perspective," *Frontiers in Pharmacology*, vol. 11, Article ID 586548, 2021.

[55] N. Basavegowda, J. K. Patra, and K.-H. Baek, "Essential oils and mono/bi/tri-metallic nanocomposites as alternative sources of antimicrobial agents to combat multidrug-resistant microorganisms: an overview," *Molecules*, vol. 25, no. 5, Article ID 1058, 2020.

[56] A. V. Rane, K. Kanny, V. K. Abitha, and S. Thomas, "Methods for synthesis of nanoparticles and fabrication of nanocomposites," in *Synthesis of Inorganic Nanomaterials*, pp. 121–139, Elsevier, 2018.

[57] R. K. Sharma and R. Ghose, "Synthesis of nanocrystalline CuO–ZnO mixed metal oxide powder by a homogeneous precipitation method," *Ceramics International*, vol. 40, no. 7, Part B, pp. 10919–10926, 2014.

[58] M. A. Subhan, N. Uddin, P. Sarker, A. K. Azad, and K. Begum, "Photoluminescence, photocatalytic and antibacterial activities of $CeO_2 \cdot CuO \cdot ZnO$ nanocomposite fabricated by co-precipitation method," *Spectrochimica Acta Part A: Molecular and Biomolecular Spectroscopy*, vol. 149, pp. 839–850, 2015.

[59] M. A. Subhan, T. Ahmed, N. Uddin, A. K. Azad, and K. Begum, "Synthesis, characterization, PL properties, photocatalytic and antibacterial activities of nano multi-metal oxide $NiO \cdot CeO_2 \cdot ZnO$," *Spectrochimica Acta Part A: Molecular and Biomolecular Spectroscopy*, vol. 136, Part B, pp. 824–831, 2015.

[60] S. Sudhaparimala and M. Vaishnavi, "Biological synthesis of nano composite SnO_2-ZnO–screening for efficient photocatalytic degradation and antimicrobial activity," *Materials Today: Proceedings*, vol. 3, no. 6, pp. 2373–2380, 2016.

[61] R. Mohammadi-Aloucheh, A. Habibi-Yangjeh, A. Bayrami, S. Latifi-Navid, and A. Asadi, "Enhanced anti-bacterial activities of ZnO nanoparticles and ZnO/CuO nanocomposites synthesized using *Vaccinium arctostaphylos* L. fruit extract," *Artificial Cells, Nanomedicine, and Biotechnology*, vol. 46, no. sup1, pp. 1200–1209, 2018.

[62] D. Saravanakkumar, S. Sivaranjani, K. Kaviyarasu et al., "Synthesis and characterization of ZnO–CuO nanocomposites powder by modified perfume spray pyrolysis method and its antimicrobial investigation," *Journal of Semiconductors*, vol. 39, no. 3, Article ID 033001, 2018.

[63] K. Karthik, S. Dhanuskodi, C. Gobinath, S. Prabukumar, and S. Sivaramakrishnan, "Multifunctional properties of microwave assisted CdO–NiO–ZnO mixed metal oxide nanocomposite: enhanced photocatalytic and antibacterial activities," *Journal of Materials Science: Materials in Electronics*, vol. 29, pp. 5459–5471, 2018.

[64] M. ur-Rehman, W. Rehman, M. Waseem et al., "Fabrication of titanium-tin oxide nanocomposite with enhanced adsorption and antimicrobial applications," *Journal of Chemical & Engineering Data*, vol. 64, no. 6, pp. 2436–2444, 2019.

[65] K. E. Rakesh, M. V. Vyshnavi, and R. Antony, "Photodegradation and antibacterial properties of zeolite cerium oxide nanocomposite," *AIP Conference Proceedings*, vol. 2162, no. 1, Article ID 020164, 2019.

[66] M. R. Abhilash, G. Akshatha, and S. Srikantaswamy, "Photocatalytic dye degradation and biological activities of the Fe_2O_3/Cu_2O nanocomposite," *RSC Advances*, vol. 9, no. 15, pp. 8557–8568, 2019.

[67] Y. L. Ying, S. Y. Pung, S. Sreekantan, Y. F. Yee, M. T. Ong, and Y. F. Pung, "Structural and antibacterial properties of WO_3/ZnO hybrid particles against pathogenic bacteria," *Materials Today: Proceedings*, vol. 17, Part 3, pp. 1008–1017, 2019.

[68] H. B. Gasmalla, X. Lu, M. I. Shinger, L. Ni, A. N. Chishti, and G. Diao, "Novel magnetically separable of $Fe_3O_4/Ag_3PO_4@WO_3$ nanocomposites for enhanced photocatalytic and antibacterial activity against *Staphylococcus aureus* (*S. aureus*)," *Journal of Nanobiotechnology*, vol. 17, Article ID 58, 2019.

[69] T. Jan, S. Azmat, Q. Mansoor et al., "Superior antibacterial activity of ZnO–CuO nanocomposite synthesized by a chemical co-precipitation approach," *Microbial Pathogenesis*, vol. 134, Article ID 103579, 2019.

[70] P. Panchal, D. R. Paul, A. Sharma et al., "Phytoextract mediated ZnO/MgO nanocomposites for photocatalytic and

antibacterial activities," *Journal of Photochemistry and Photobiology A: Chemistry*, vol. 385, Article ID 112049, 2019.

[71] N. Pandiyan, B. Murugesan, J. Sonamuthu, S. Samayanan, and S. Mahalingam, "[BMIM] PF$_6$ ionic liquid mediated green synthesis of ceramic SrO/CeO$_2$ nanostructure using *Pedalium murex* leaf extract and their antioxidant and antibacterial activities," *Ceramics International*, vol. 45, no. 9, pp. 12138–12148, 2019.

[72] T. Munawar, S. Yasmeen, M. Hasan et al., "Novel tri-phase heterostructured ZnO–Yb$_2$O$_3$–Pr$_2$O$_3$ nanocomposite; structural, optical, photocatalytic and antibacterial studies," *Ceramics International*, vol. 46, no. 8, Part A, pp. 11101–11114, 2020.

[73] M. Ahmad, S. J. A. Zaidi, S. Zoha et al., "Pseudo-SILAR assisted unique synthesis of ZnO/Ag$_2$O nanocomposites for improved photocatalytic and antibacterial performance without cytotoxic effect," *Colloids and Surfaces A: Physicochemical and Engineering Aspects*, vol. 603, Article ID 125200, 2020.

[74] K. Kannan, D. Radhika, M. P. Nikolova, V. Andal, K. K. Sadasivuni, and L. S. Krishna, "Facile microwave-assisted synthesis of metal oxide CdO–CuO nanocomposite: photocatalytic and antimicrobial enhancing properties," *Optik*, vol. 218, Article ID 165112, 2020.

[75] A. Syed, L. S. R. Yadav, A. H. Bahkali, A. M. Elgorban, D. Abdul Hakeem, and N. Ganganagappa, "Effect of CeO$_2$/ZnO nanocomposite for photocatalytic and antibacterial activities," *Crystals*, vol. 10, no. 9, Article ID 817, 2020.

[76] S. Sunaryono, S. N. Halizah, S. Zulaikah, H. Susanto, N. Mufti, and A. Taufiq, "Contribution of ZnO/TiO$_2$ nanocomposite particles towards bacterial growth inhibition," *AIP Conference Proceedings*, vol. 2353, Article ID 030013, 2021.

[77] K. I. Dhanalekshmi, M. J. Umapathy, P. Magesan, and X. Zhang, "Biomaterial (Garlic and Chitosan)-doped WO$_3$–TiO$_2$ hybrid nanocomposites: their solar light photocatalytic and antibacterial activities," *ACS Omega*, vol. 5, no. 49, pp. 31673–31683, 2020.

[78] K. Kannan, D. Radhika, D. Gnanasangeetha et al., "Photocatalytic and antimicrobial properties of microwave synthesized mixed metal oxide nanocomposite," *Inorganic Chemistry Communications*, vol. 125, Article ID 108429, 2021.

[79] K. Kannan, D. Radhika, D. Gnanasangeetha, L. S. Krishna, and K. Gurushankar, "Y^{3+} and Sm^{3+} co-doped mixed metal oxide nanocomposite: structural, electrochemical, photocatalytic, and antibacterial properties," *Applied Surface Science Advances*, vol. 4, Article ID 100085, 2021.

[80] K. Kannan, D. Radhika, K. R. Reddy et al., "Gd^{3+} and Y^{3+} co-doped mixed metal oxide nanohybrids for photocatalytic and antibacterial applications," *Nano Express*, vol. 2, no. 1, Article ID 010014, 2021.

[81] V. N. L. Uyen, N. T. T. Van, N. Van Minh, T. Nguyen, and H. K. P. Ha, "Fabrication of Cu$_2$O–ZnO Nanocomposite by the sol-gel technique and its antibacterial activity," *Journal of Biochemical Technology*, vol. 11, no. 1, pp. 18–24, 2020.

[82] F. Mukhtar, T. Munawar, M. S. Nadeem et al., "Multi metal oxide NiO–Fe$_2$O$_3$–CdO nanocomposite-synthesis, photocatalytic and antibacterial properties," *Applied Physics A*, vol. 126, Article ID 588, 2020.

[83] M. I. Rahmah, N. M. Saadoon, A. J. Mohasen, R. I. Kamel, T. A. Fayad, and N. M. Ibrahim, "Double hydrothermal synthesis of iron oxide/silver oxide nanocomposites with antibacterial activity," *Journal of the Mechanical Behavior of Materials*, vol. 30, no. 1, pp. 207–212, 2021.

[84] D. A. Al Farraj, A. M. Al-Mohaimeed, R. M. Alkufeidy, and N. A. Alkubaisi, "Facile synthesis and characterization of CeO$_2$–Al$_2$O$_3$ nano-heterostructure for enhanced visible-light photocatalysis and bactericidal applications," *Colloid and Interface Science Communications*, vol. 41, Article ID 100375, 2021.

[85] R. Gandotra, Y.-R. Chen, T. Murugesan, T.-W. Chang, H.-Y. Chang, and H.-N. Lin, "Highly efficient and morphology dependent antibacterial activities of photocatalytic Cu$_x$O/ZnO nanocomposites," *Journal of Alloys and Compounds*, vol. 873, Article ID 159769, 2021.

[86] M. Noor, M. A. Al Mamun, A. K. M. Atique Ullah et al., "Physics of Ce^{3+}↔Ce^{4+} electronic transition in phytosynthesized CeO$_2$/CePO$_2$ nanocomposites and its antibacterial activities," *Journal of Physics and Chemistry of Solids*, vol. 148, Article ID 109751, 2021.

[87] N. S. Bisht, A. H. Tripathi, S. Kumar, S. P. S. Mehta, and A. Dandapat, "Silver oxide-bismuth oxybromide nanocomposites as an excellent weapon to combat with opportunistic human pathogens," *Journal of Photochemistry and Photobiology*, vol. 6, Article ID 100031, 2021.

[88] S. J. Owonubi, N. M. Malima, and N. Revaprasadu, "Metal oxide-based nanocomposites as antimicrobial and biomedical agents," in *Antibiotic Materials in Healthcare*, pp. 287–323, Elsevier, 2020.

[89] T. Ghosh, A. B. Das, B. Jena, and C. Pradhan, "Antimicrobial effect of silver zinc oxide (Ag-ZnO) nanocomposite particles," *Frontiers in Life Science*, vol. 8, no. 1, pp. 47–54, 2015.

[90] S. Kulkarni, M. Jadhav, P. Raikar, D. A. Barretto, S. K. Vootla, and U. S. Raikar, "Green synthesized multifunctional Ag@Fe$_2$O$_3$ nanocomposites for effective antibacterial, antifungal and anticancer properties," *New Journal of Chemistry*, vol. 41, no. 17, pp. 9513–9520, 2017.

[91] E. B. Tibayan Jr, M. A. Muflikhun, V. Kumar, C. Fisher, C. V. Al Rey, and G. N. C. Santos, "Performance evaluation of Ag/SnO$_2$ nanocomposite materials as coating material with high capability on antibacterial activity," *Ain Shams Engineering Journal*, vol. 11, no. 3, pp. 767–776, 2020.

[92] S. Shams, A. U. Khan, Q. Yuan et al., "Facile and eco-benign synthesis of Au@Fe$_2$O$_3$ nanocomposite: efficient photocatalytic, antibacterial and antioxidant agent," *Journal of Photochemistry and Photobiology B: Biology*, vol. 199, Article ID 111632, 2019.

[93] M. Hassanpour, M. Salavati-Niasari, S. A. H. Tafreshi, H. Safardoust-Hojaghan, and F. Hassanpour, "Synthesis, characterization and antibacterial activities of Ni/ZnO nanocomposites using bis (salicylaldehyde) complex precursor," *Journal of Alloys and Compounds*, vol. 788, pp. 383–390, 2019.

[94] M. A. Muflikhun, R. K. Adi, and G. N. Santos, "Nanocomposite material synthesized via horizontal vapor phase growth technique: evaluation and application perspective," in *21st Century Nanostructured Materials - Physics, Chemistry, Classification, and Emerging Applications in Industry, Biomedicine, and Agriculture*, IntechOpen, 2021.

[95] A. U. Khan, A. ur Rahman, Q. Yuan et al., "Facile and eco-benign fabrication of Ag/Fe$_2$O$_3$ nanocomposite using *Algaia Monozyga* leaves extract and its' efficient biocidal and photocatalytic applications," *Photodiagnosis and Photodynamic Therapy*, vol. 32, Article ID 101970, 2020.

[96] A. Saranya, A. Thamer, K. Ramar et al., "Facile one pot microwave-assisted green synthesis of Fe₂O₃/Ag nanocomposites by phytoreduction: potential application as sunlight-driven photocatalyst, antibacterial and anticancer agent," *Journal of Photochemistry and Photobiology B: Biology*, vol. 207, Article ID 111885, 2020.

[97] R. B. Asamoah, E. Annan, B. Mensah et al., "A comparative study of antibacterial activity of CuO/Ag and ZnO/Ag nanocomposites," *Advances in Materials Science and Engineering*, vol. 2020, Article ID 7814324, 18 pages, 2020.

[98] D. Bhardwaj and R. Singh, "Green biomimetic synthesis of Ag–TiO₂ nanocomposite using *Origanum majorana* leaf extract under sonication and their biological activities," *Bioresources and Bioprocessing*, vol. 8, Article ID 1, 2021.

[99] P. G. Bhavyasree and T. S. Xavier, "A critical green biosynthesis of novel CuO/C porous nanocomposite via the aqueous leaf extract of *Ficus religiosa* and their antimicrobial, antioxidant, and adsorption properties," *Chemical Engineering Journal Advances*, vol. 8, Article ID 100152, 2021.

[100] M. A. Tofighy and T. Mohammadi, "Carbon nanotubes-polymer nanocomposite membranes for pervaporation," in *Polymer Nanocomposite Membranes for Pervaporation*, pp. 105–133, Elsevier, 2020.

[101] M. R. Mansor and M. Z. Akop, "Polymer nanocomposites smart materials for energy applications," in *Polymer Nanocomposite-Based Smart Materials*, pp. 157–176, Elsevier, 2020.

[102] P. Dimitrakellis, G. D. Kaprou, G. Papavieros et al., "Enhanced antibacterial activity of ZnO-PMMA nanocomposites by selective plasma etching in atmospheric pressure," *Micro and Nano Engineering*, vol. 13, Article ID 100098, 2021.

[103] A. Sanmugam, D. Vikraman, H. J. Park, and H.-S. Kim, "One-pot facile methodology to synthesize chitosan-ZnO-graphene oxide hybrid composites for better dye adsorption and antibacterial activity," *Nanomaterials*, vol. 7, no. 11, Article ID 363, 2017.

[104] Y. Gutha, J. L. Pathak, W. Zhang, Y. Zhang, and X. Jiao, "Antibacterial and wound healing properties of chitosan/poly (vinyl alcohol)/zinc oxide beads (CS/PVA/ZnO)," *International Journal of Biological Macromolecules*, vol. 103, pp. 234–241, 2017.

[105] C. Liu, J. Shen, C. Z. Liao, K. W. K. Yeung, and S. C. Tjong, "Novel electrospun polyvinylidene fluoride-graphene oxide-silver nanocomposite membranes with protein and bacterial antifouling characteristics," *eXPRESS Polymer Letters*, vol. 12, no. 4, pp. 365–382, 2018.

[106] M. Beiranvand, S. Farhadi, and A. Mohammadi, "Graphene Oxide/Hydroxyapatite/Silver (rGO/HAP/Ag) nanocomposite: synthesis, characterization, catalytic and antibacterial activity," *International Journal of Nano Dimension*, vol. 10, no. 2, pp. 180–194, 2019.

[107] D. Bharathi, R. Ranjithkumar, B. Chandarshekar, and V. Bhuvaneshwari, "Preparation of chitosan coated zinc oxide nanocomposite for enhanced antibacterial and photocatalytic activity: as a bionanocomposite," *International Journal of Biological Macromolecules*, vol. 129, pp. 989–996, 2019.

[108] K. D. Dejen, E. A. Zereffa, H. C. A. Murthy, and A. Merga, "Synthesis of ZnO and ZnO/PVA nanocomposite using aqueous moringa oleifeira leaf extract template: antibacterial and electrochemical activities," *Reviews on Advanced Materials Science*, vol. 59, no. 1, pp. 464–476, 2020.

[109] C. N. Nandana, M. Christeena, and D. Bharathi, "Synthesis and characterization of chitosan/silver nanocomposite using rutin for antibacterial," *Journal of Cluster Science*, vol. 33, pp. 269–279, 2022.

[110] T. K. Jana, S. K. Maji, A. Pal, R. P. Maiti, T. K. Dolai, and K. Chatterjee, "Photocatalytic and antibacterial activity of cadmium sulphide/zinc oxide nanocomposite with varied morphology," *Journal of Colloid and Interface Science*, vol. 480, pp. 9–16, 2016.

[111] S. Archana, K. Y. Kumar, B. K. Jayanna et al., "Versatile graphene oxide decorated by star shaped Zinc oxide nanocomposites with superior adsorption capacity and antimicrobial activity," *Journal of Science: Advanced Materials and Devices*, vol. 3, no. 2, pp. 167–174, 2018.

[112] N. El-Shafai, M. E. El-Khouly, M. El-Kemary, M. Ramadan, I. Eldesoukey, and M. Masoud, "Graphene oxide decorated with zinc oxide nanoflower, silver and titanium dioxide nanoparticles: fabrication, characterization, DNA interaction, and antibacterial activity," *RSC Advances*, vol. 9, no. 7, pp. 3704–3714, 2019.

[113] P. G. Bhavyasree and T. S. Xavier, "Green synthesis of Copper Oxide/Carbon nanocomposites using the leaf extract of *Adhatoda vasica* nees, their characterization and antimicrobial activity," *Heliyon*, vol. 6, no. 2, Article ID e03323, 2020.

[114] G. Sharma, D. Prema, K. S. Venkataprasanna, J. Prakash, S. Sahabuddin, and G. D. Venkatasubbu, "Photo induced antibacterial activity of CeO₂/GO against wound pathogens," *Arabian Journal of Chemistry*, vol. 13, no. 11, pp. 7680–7694, 2020.

[115] A.-Z. Warsi, F. Aziz, S. Zulfiqar, S. Haider, I. Shakir, and P. O. Agboola, "Synthesis, characterization, photocatalysis, and antibacterial study of WO₃, MXene and WO₃/MXene nanocomposite," *Nanomaterials*, vol. 12, no. 4, Article ID 713, 2022.

[116] M. U. Munir, A. Ahmed, M. Usman, and S. Salman, "Recent advances in nanotechnology-aided materials in combating microbial resistance and functioning as antibiotics substitutes," *International Journal of Nanomedicine*, vol. 15, pp. 7329–7358, 2020.

[117] D. A. Dik, J. F. Fisher, and S. Mobashery, "Cell-wall recycling of the gram-negative bacteria and the nexus to antibiotic resistance," *Chemical Reviews*, vol. 118, no. 12, pp. 5952–5984, 2018.

[118] T. J. Silhavy, D. Kahne, and S. Walker, "The bacterial cell envelope," *Cold Spring Harbor Perspectives in Biology*, vol. 2, no. 5, Article ID a000414, 2010.

[119] X. Xiao, Z.-C. Wu, K.-C. Chou, and F. Fraternali, "A multi-label classifier for predicting the subcellular localization of gram-negative bacterial proteins with both single and multiple sites," *PLoS ONE*, vol. 6, no. 6, Article ID e20592, 2011.

[120] A. Wada, M. Kono, S. Kawauchi, Y. Takagi, T. Morikawa, and K. Funakoshi, "Rapid discrimination of Gram-positive and Gram-negative bacteria in liquid samples by using NaOH-sodium dodecyl sulfate solution and flow cytometry," *PLoS ONE*, vol. 7, no. 10, Article ID e47093, 2012.

[121] A. Dehzangi, S. Sohrabi, R. Heffernan et al., "Gram-positive and gram-negative subcellular localization using rotation forest and physicochemical-based features," *BMC Bioinformatics*, vol. 16, no. S4, Article ID S1, 2015.

[122] S. Gharpure and B. Ankamwar, "Synthesis and antimicrobial properties of zinc oxide nanoparticles," *Journal of Nanoscience and Nanotechnology*, vol. 20, no. 10, pp. 5977–5996, 2020.

[123] N. Widiarti, J. K. Sae, and S. Wahyuni, "Synthesis CuO–ZnO nanocomposite and its application as an antibacterial agent," *IOP Conference Series: Materials Science and Engineering*, vol. 172, Article ID 012036, 2017.

[124] M. Maulidiyah, P. E. Susilowati, N. K. Mudhafar et al., "Photo-inactivation *Staphylococcus aureus* by using formulation of Mn–N–TiO_2 composite coated wall paint," *Biointerface Research in Applied Chemistry*, vol. 12, no. 2, pp. 1628–1637, 2022.

[125] Z. Kanwal, M. A. Raza, S. Riaz et al., "Synthesis and characterization of silver nanoparticle-decorated cobalt nanocomposites (Co@AgNPs) and their density-dependent antibacterial activity," *Royal Society Open Science*, vol. 6, no. 5, Article ID 182135, 2019.

[126] N. L. U. Vo, T. T. Van Nguyen, T. Nguyen et al., "Antibacterial shoe insole-coated CuO–ZnO nanocomposite synthesized by the sol-gel technique," *Journal of Nanomaterials*, vol. 2020, Article ID 8825567, 13 pages, 2020.

[127] R. Abedinpour Farahmand, F. Raouf, S. Hamedi, and N. Gilani, "Investigation on antibacterial activity of alpha Fe_2O_3/ZnO nanocomposites against Gram-positive and Gram-negative bacteria," *Materials Technology*, vol. 37, no. 12, pp. 2265–2275, 2022.

[128] T. Ghosh, A. Chattopadhyay, S. Pramanik et al., "Role of Ag nanoparticles on photoluminescence emissions, antibacterial activities, and photocatalytic effects in ZnO–Ag nanocomposites synthesized via low temperature green synthesis method using azadirachta Indica leaf extract," *Materials Technology*, vol. 37, no. 12, pp. 2300–2312, 2022.

[129] S. Ebrahimiasl, A. Zakaria, A. Kassim, and S. N. Basri, "Novel conductive polypyrrole/zinc oxide/chitosan bionanocomposite: synthesis, characterization, antioxidant, and antibacterial activities," *International Journal of Nanomedicine*, vol. 10, no. 1, pp. 217–227, 2015.

[130] S. A. Rajan, A. Khan, S. Asrar, H. Raza, R. K. Das, and N. K. Sahu, "Synthesis of ZnO/Fe_3O_4/rGO nanocomposites and evaluation of antibacterial activities towards *E. coli* and *S. aureus*," *IET Nanobiotechnology*, vol. 13, no. 7, pp. 682–687, 2019.

[131] M. Bhushan, Y. Kumar, L. Periyasamy, and A. K. Viswanath, "Fabrication and a detailed study of antibacterial properties of alpha Fe_2O_4/NiO nanocomposites along with their structural, optical, thermal, magnetic and cytotoxic features," *Nanotechnology*, vol. 30, no. 18, Article ID 185101, 2019.

[132] M. Pandey, M. Singh, K. Wasnik et al., "Targeted and enhanced antimicrobial inhibition of mesoporous ZnO-Ag_2O/Ag, ZnO–CuO, and ZnO–SnO_2 composite nanoparticles," *ACS Omega*, vol. 6, no. 47, pp. 31615–31631, 2021.